Electronic Supplementary Material (ESI) for Chemical Science.
This journal is © The Royal Society of Chemistry 2019

Electronic Supplemental Information (ESI)

DOI

Turn on of Sky-Blue Thermally Activated Delayed Fluorescence and Circularly Polarized Luminescence (CPL) via Increased Torsion by a Bulky Carbazolophane Donor

Nidhi Sharma,†[a,b] Eduard Spuling,†[c] Cornelia M. Mattern,[c] Wenbo Li,[b] Olaf Fuhr,[d] Youichi Tsuchiya,[e,f] Chihaya Adachi,[e,f,g,h] Stefan Bräse,*[c,d] Ifor D. W. Samuel,*[b] and Eli Zysman-Colman*[a]

[a.] *Organic Semiconductor Centre, EaStCHEM School of Chemistry, University of St Andrews, St Andrews, Fife, KY16 9ST, UK*
E-mail: eli.zysman-colman@st-andrews.ac.uk

[b.] *Organic Semiconductor Centre, SUPA, School of Physics and Astronomy, University of St Andrews, North Haugh, St Andrews, KY16 9SS, UK*
E-mail: idws@st-andrews.ac.uk.

[c.] *Institute of Organic Chemistry (IOC), Karlsruhe Institute of Technology (KIT), Fritz-Haber-Weg 6, 76131 Karlsruhe, Germany*
E-mail: braese@kit.edu.

[d.] *Institute of Toxicology and Genetics (ITG), Karlsruhe Institute of Technology (KIT), Hermann-von-Helmholtz-Platz 1, D-76344 Eggenstein-Leopoldshafen, Germany*

[e.] *Center for Organic Photonics and Electronics Research (OPERA), Kyushu University, 744 Motooka, Nishi-ku, Fukuoka 819-0395, Japan.*

[f.] *JST, ERATO, Adachi Molecular Exciton Engineering Project, Kyushu University, 744 Motooka, Nishi-ku, Fukuoka 819-0395, Japan.*

[g.] *Department of Chemistry and Biochemistry, Kyushu University, 744 Motooka, Nishi-ku, Fukuoka 819-0395, Japan.*

[h.] *International Institute for Carbon Neutral Energy Research (WPI-I2CNER), Kyushu University, 744 Motooka, Nishi-ku, Fukuoka 819-0395, Japan.*

† Nidhi Sharma and Eduard Spuling contributed equally to this work.

Electronic Supplementary Information (ESI) available: [details of any supplementary information available should be included here]. See DOI: 10.1039/x0xx00000x

Table of Contents

1. Prior Literature examples on CPL active TADF materials 2
2. General Experimental Information 3
3. Nomenclature of [2.2]Paracyclophanes 5
4. Synthesis of Compounds 6
5. Chiral Separation and Determination of Alsolute Configuration 18
6. Crystallography 20
7. Electrochemical Characterization. 21
8. Thermal Analysis. 21
9. Photophysical Characterization. 22
10. DFT modelling 25
11. Device Characterization. 29
12. References 30

1. Prior Literature examples on CPL active TADF materials

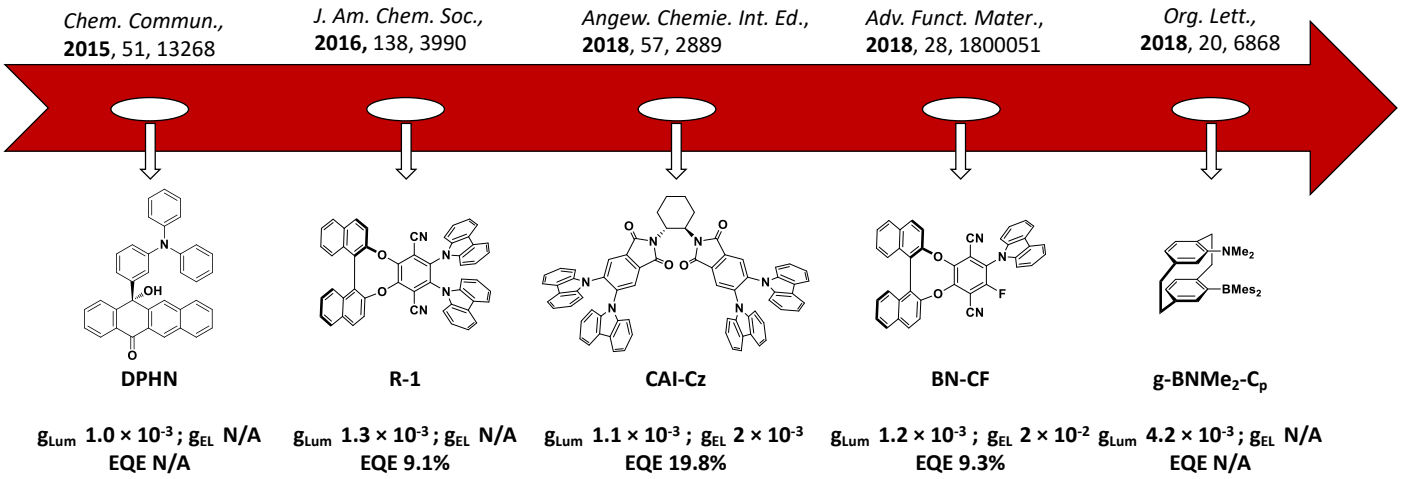

Figure **S1**. Prior literature examples of CPL active TADF materials.

2. General Experimental Information

The NMR spectra of compounds described herein were recorded by a Bruker Avance 300 NMR instrument at 300 MHz for ^{1}H NMR and 75 MHz for ^{13}C NMR, a Bruker Avance 400 NMR instrument at 400 MHz for ^{1}H NMR and 101 MHz for ^{13}C NMR or a Bruker Avance 500 NMR instrument at 500 MHz for ^{1}H NMR, 125 MHz for ^{13}C NMR and 470 MHz for ^{19}F NMR.

The NMR spectra were recorded at room temperature in deuterated solvents commercially acquired from Eurisotop. The chemical shift δ is displayed in parts per million [ppm] and the references used were the ^{1}H and ^{13}C peaks of the solvents themselves: d_1-chloroform ($CDCl_3$): 7.26 ppm for ^{1}H and 77.0 ppm for ^{13}C), d_6-dimethyl sulfoxide (DMSO-d_6): 2.50 ppm for ^{1}H and 39.4 ppm for ^{13}C.

Evaluation of the signals was done according to first order spectra. For the characterization of centrosymmetric signals, the signal's median point was chosen, for multiplets the signal range. The following abbreviations were used to describe couplings: d = doublet, t = triplet, m = multiplet, dd = doublet of doublet, ddd = doublet of doublet of doublet, dt = doublet of triplet. Coupling constants "*J*" are given in Hertz [Hz] in absolute value with the largest value first. Couplings are given with their respective number of bindings and binding partners, as far as they could be determined, written as index of the coupling constants. Signals of the ^{13}C spectrum were assigned with the help of *distortionless enhancement by polarization transfer* spectra DEPT90 and DEPT135 and were specified in the following way: DEPT: + = primary or tertiary carbon atoms (positive DEPT signal), – = secondary carbon atoms (negative DEPT signal), C_{quat} = quaternary carbon atoms (no DEPT signal).

The infrared spectra were recorded with an instrument made by Bruker, model IFS 88. Solids were measured by attenuated total reflection (ATR method). Absorption is given in wave numbers $\bar{\upsilon}$ [cm^{-1}] and was measured in the range from 3600 cm^{-1} to 500 cm^{-1}. Characterization of the absorption bands was done in sequence of transmission strength T with following abbreviations: vs (very strong, 0−9% T), s (strong, 10−39% T), m (medium, 40−69% T), w (weak, 70−89% T), vw (very weak, 90−100% T) and br (broad).

The electron ionization (EI) and fast atom bombardment (FAB) methods were conducted using an instrument by Finnigan, model MAT 90 (70 eV), was used with 3-nitrobenzyl alcohol (3-NBA) as matrix and reference for high resolution. For the interpretation of the spectra, molecular peaks $[M]^+$, peaks of pseudo molecules $[M+H]^+$ and characteristic fragment peaks are indicated with their mass to charge ratio (*m/z*) and in case of EI their intensity in percent, relative to the base peak (100%) is given. In the case of high resolution measurements, the tolerated error is 0.0005 m/z.

APCI and ESI methods were recorded on a Q Exactive (Orbitrap) mass spectrometer (Thermo Fisher Scientific, San Jose, CA, USA) equipped with a HESI II probe to record high resolution. The tolerated error is 5 ppm of the molecular mass. Again, the spectra were interpreted by molecular peaks $[M]^+$, peaks of pseudo molecules $[M+H]^+$ and characteristic fragment peaks and indicated with their mass to charge ratio (*m/z*).

For the analytical thin layer chromatography, TLC silica plates coated with fluorescence indicator, made by Merck (Art. Nr. 105554, silica gel 60 F254, thickness 0.2 mm) were used. UV active compounds were detected with a Heraeus UV-lamp, model Fluotest, at 254 nm and 366 nm wavelength.

Solvents of p.a. quality (per analysis) were commercially acquired from Sigma Aldrich, Carl Roth or Acros Fisher Scientific and, unless otherwise stated, used without previous purification. Absolutized solvents were either purchased from Carl Roth, Acros or Sigma Aldrich (< 50 ppm H_2O over molecular sieve).

All reagents were commercially acquired (through ABCR, Acros, Alfa Aesar or Sigma Aldrich) or were available in the working group. Unless otherwise stated, they were used without further purification. Elemental analysis was done with an Elementar vario MICRO instrument. The weight scale used was a Sartorius M2P. Calculated (calc.) and found values for carbon, hydrogen and nitrogen are indicated in fractions of 100% mass.

3. Nomenclature of [2.2]Paracyclophanes

The IUPAC nomenclature for cyclophanes in general is rather confusing. Therefore Vögtle *et al.* developed a specific cyclophane nomenclature, which is based on a core-substituent ranking.[1] This is exemplified in Figure **S2** for the [2.2]paracyclophane.

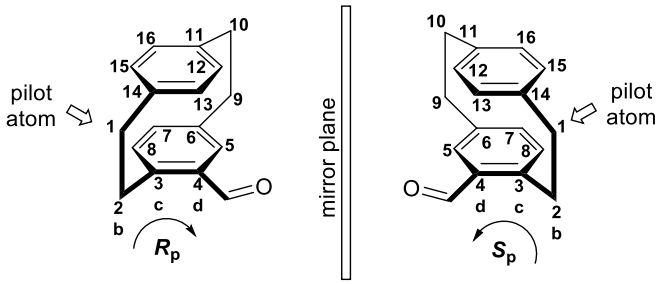

Figure **S2**. Nomenclature illustrated on the enantiomers of 4-formyl[2.2]paracyclophane.

The core structure is named according to the length of the aliphatic bridges in squared brackets (e.g. [n.m]) and the benzene substitution patterns (*ortho*, *meta* or *para*). [2.2]Paracyclophane belongs to the D_{2h} symmetry, which is broken by the first substituent, resulting in two planar chiral enantiomers. They cannot be drawn in a racemic fashion. By definition, the arene bearing the substituent is set to a chirality plane, and the first atom of the cyclophane structure outside the plane and closest to the chirality center is defined as the "*pilot atom*". If both arenes are substituted, the substituent with higher priority according to the Cahn-Ingold-Prelog (CIP) nomenclature is preferred.[2] The stereo descriptor is determined by the sense of rotation viewed from the pilot atom. To describe the positions of the substituents correctly, an unambiguous numeration is needed. The numbering of the arenes follows the sense of rotation determined by CIP. To indicate the stereochemistry of the planar chirality, a subscripted *p* is added.

In this work, chiral heterocycle-fused derivatives are presented. In this case the cyclophane, and the carbazole nomenclatures are exerted simultaneously (Figure **S3**).

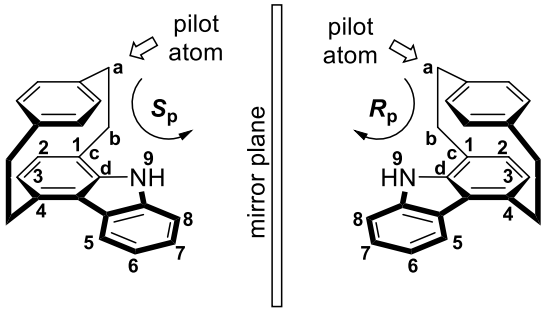

Figure **S3**. Nomenclature of the [2]paracyclo[2](1,4)carbazolophane (short: carbazolophane, Czp).

The first report of the [2]paracyclo[2](1,4)carbazolophane (**Czp**) by Bolm *et al.*[3] presented the nomenclature, but no information on chirality was given The stereo descriptors follow the same standard as reported for the [2.2]paracyclophane. If viewed as a disubstituted [2.2]paracyclophane, then the nitrogen is assigned a higher priority than the carbon substituent, resulting in the respective sense of numbering as depicted in red.

4. Synthesis of Compounds

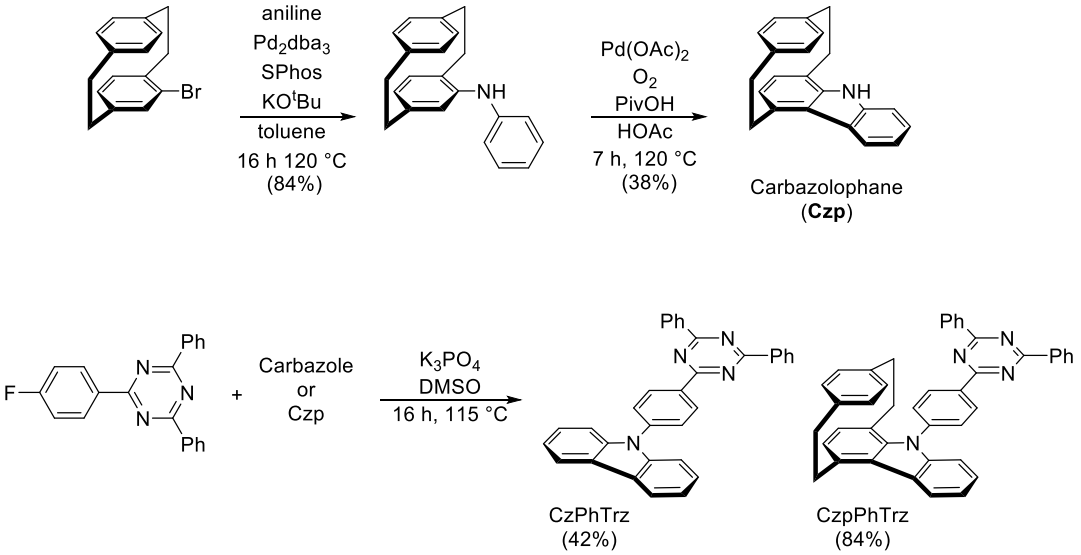

Scheme **S1**. Synthetic overview. Synthesis of the carbazolophane published by Bolm *et al.*[4]

Air-sensitive and moisture-sensitive reactions were carried out under argon atmosphere in previously baked out apparatuses with standard Schlenk techniques. Solid compounds were ground using a mortar and pestle before the reaction, liquid reagents and solvents were injected with plastic syringes and stainless-steel cannula of different sizes, unless otherwise specified.

Reactions at low temperatures were cooled using shallow vacuum flasks produced by Isotherm, Karlsruhe, filled with a water/ice mixture for 0 °C, water/ice/sodium chloride for –20 °C or isopropanol/dry ice mixture for –78 °C. In reactions at high temperatures, the reaction flask was equipped with a reflux condenser and connected to the argon line.

Solvents were evaporated under reduced pressure at the lowest possible temperature (40 °C) using a rotary evaporator. Unless otherwise stated, solutions of inorganic salts are saturated aqueous solutions.

The progression of the reaction in the liquid phase was monitored via TLC. UV active compounds were detected with a UV-lamp at 254 nm and 366 nm wavelength. Depending on the confronted problem, the detection was carried out with vanillin solution, potassium permanganate solution or bromocresol green-methanol solution followed by heating using a heat gun. Additionally, low resolution APCI-MS (atmospheric pressure chemical ionization mass spectrometry) was recorded with a device from Advion expression CMS in positive mode with a single quadrupole mass analyzer. The observed molecule ion is interpreted as $[M+H]^+$. Unless otherwise stated, the crude compounds were purified by flash chromatography. For the stationary phase of the column, silica gel, produced by Merck (silica gel 60, 0.040 × 0.063 mm, 260 – 400 mesh ASTM), and sea sand by Riedel de Haën (baked out and washed with hydrochloric acid) were used. Solvents used were commercially acquired in HPLC-grade and individually measured volumetrically before mixing.

***rac*-4-Bromo[2.2]paracyclophane**

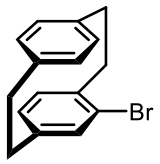

To 80.4 mg of iron filings (1.44 mmol, 2 mol%) provided in a 500 mL three neck flask equipped with a reflux condenser, 5 mL of a solution consisting of 3.77 mL of bromine (11.8 g, 73.7 mmol, 1.02 equiv.) in 80 mL of dichloromethane prepared in a dropping funnel were added and stirred for 1 h at room temperature. Afterwards, 15.0 g of [2.2]paracyclophane (72.0 mmol, 1.00 equiv.) and 250 mL dichloromethane were added, and the mixture was stirred for 30 min. The remaining bromine solution was then added dropwise over a period of 4 h and the mixture was stirred for 2 d. The reaction was quenched with 200mL of saturated sodium sulfite solution and stirred for another 1.5 h until full discoloration of the reaction mixture. Then, the separated organic phase was washed with 200 mL of brine and dried over Na_2SO_4. The solvent was evaporated under reduced pressure to yield 18.2 g (88%, 63.4 mmol) of a white solid. – $\mathbf{R_f}$ = 0.63 (cyclohexane:ethyl acetate 50:1) – **^{1}H NMR** (400 MHz, $CDCl_3$) δ [ppm] = 7.19 (dd, $^3J_{HH}$ = 7.9 Hz, $^4J_{HH}$ = 2.0 Hz, 1H), 6.58 (dd, $^3J_{HH}$ = 7.8 Hz, $^4J_{HH}$ = 2.0 Hz, 1H), 6.56 – 6.52 (m, 2H), 6.52 – 6.45 (m, 3H), 3.48 (ddd, $^3J_{HH}$ = 13.0 Hz, $^3J_{HH}$ = 10.1 Hz, $^4J_{HH}$ = 2.2 Hz, 1H), 3.22 (ddd, $^3J_{HH}$ = 13.1 Hz, $^3J_{HH}$ = 10.1 Hz, $^4J_{HH}$ = 6.1 Hz, 1H), 3.17 – 3.02 (m, 4H), 2.98 – 2.78 (m, 2H). – **^{13}C NMR** (101 MHz, CDCl3) δ [ppm] = 141.73 (C_{quat}, C_{Ar}), 139.43 (C_{quat}, C_{Ar}), 139.22 (C_{quat}, C_{Ar}), 137.37 (+, $C_{Ar}H$), 135.17 (+, $C_{Ar}H$), 133.43 (+, $C_{Ar}H$), 133.03 (+, $C_{Ar}H$), 132.37 (+, $C_{Ar}H$), 131.59 (+, $C_{Ar}H$), 128.81 (+, $C_{Ar}H$), 127.09 (C_{quat}, C_{Ar}), 35.98 (–, CH_2), 35.61 (–, CH_2), 34.95 (–, CH_2), 33.61 (–, CH_2). – **IR** (ATR) $\tilde{\nu}$ [cm^{-1}] = 2924 (w), 2849 (w), 1585 (w), 1541 (w), 1497 (w), 1475 (w), 1431 (w), 1408 (w), 1390 (w), 1186 (w), 1092 (vw), 1034 (m), 941 (w), 869 (w), 839 (m), 793 (w), 708 (m), 668 (w), 640 (m), 576 (w), 514 (m), 473 (w), 404 (vw), 382 (w). – **MS** (EI, 70 eV) *m/z* [%] = 288 (27) $[M(^{81}Br)]^+$, 286 (28) $[M(^{79}Br)]^+$, 184 (17) $[C_8H_7{}^{81}Br]^+$, 182 (17) $[C_8H_7{}^{79}Br]$, 104 (100) $[C_8H_8]^+$. – **HRMS** ($C_{16}H_{15}{}^{79}Br$) calc. 286.0352; found 286.0350. Analytical data matches that of the literature.[5]

***rac*-4-*N*-(Phenyl)amino[2.2]paracyclophane**

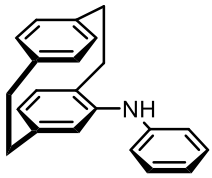

Three pressure vials were each charged with 1.15 g of *rac*-4-bromo[2.2]paracyclophane (4.00 mmol, 1.00 equiv.), 62.8 mg potassium *tert*-butoxide (5.60 mmol, 1.40 equiv.), 10.0 mg SPhos (24.0 µmol, 6 mol%) and 70.0 mg Pd_2dba_3 (80.0 µmol, 2 mol%) and evacuated and refilled with argon three times. Then 20 mL of dry toluene and 0.438 mL of aniline (628 mg, 5.60 mmol, 1.40 equiv.) were added and the mixture was stirred in argon atmosphere at 115 °C for 16 h. The dark brown crude was diluted with 50 mL of water and extracted with 50 mL of ethyl acetate. Afterwards, the organic layer was washed three times with 50 mL of saturated NH_4Cl solution and with 50 mL of brine. The organic layers were dried over Na_2SO_4 and the filtrate was evaporated under reduced pressure. The residue was purified by flash chromatography (silica, 50:1 cyclohexane:ethyl acetate) to yield 3.03 g (84%, 10.1 mmol) of a white solid. – $\mathbf{R_f}$ = 0.35 (cyclohexane:ethyl acetate 50:1) – **^{1}H NMR** (500 MHz, $CDCl_3$) δ [ppm] = 7.23 (t, $^3J_{HH}$ = 7.9 Hz, 2H), 7.01 (dd, $^3J_{HH}$ = 7.8, $^4J_{HH}$ = 1.9 Hz, 1H), 6.93 (d, $^3J_{HH}$ = 8.5 Hz, 2H), 6.87 (t, $^3J_{HH}$ = 7.3 Hz, 1H), 6.59 (dd, $^3J_{HH}$ = 7.8, $^4J_{HH}$ = 1.9 Hz, 1H), 6.51 – 6.41 (m, 3H), 6.37 (dd, $^3J_{HH}$ = 7.8, $^4J_{HH}$ = 1.8 Hz, 1H), 5.86 (d, $^3J_{HH}$ = 1.8 Hz, 1H), 5.55 (bs, 1H), 3.12 – 2.86 (m, 7H), 2.69 (ddd, $^3J_{HH}$ = 13.7, 10.1, $^2J_{HH}$ = 6.8 Hz, 1H). – **^{13}C NMR** (126 MHz, $CDCl_3$) δ [ppm] = 143.74 (C_{quat}, C_{Ar}), 141.35 (C_{quat}, C_{Ar}), 140.21 (C_{quat}, C_{Ar}), 139.64 (C_{quat}, C_{Ar}), 139.13 (C_{quat}, C_{Ar}), 135.99 (+, $C_{Ar}H$), 133.64 (+, $C_{Ar}H$), 132.85 (+, $C_{Ar}H$), 131.48 (C_{quat}, C_{Ar}), 131.34 (+, $C_{Ar}H$), 129.28 (+, $C_{Ar}H$), 127.55 (+, $C_{Ar}H$), 127.04 (+, $C_{Ar}H$), 125.99 (+, $C_{Ar}H$), 120.17 (+, $C_{Ar}H$), 116.09 (+, $C_{Ar}H$), 35.35 (–, CH_2), 35.01 (–, CH_2), 33.95 (–, CH_2), 33.93 (–, CH_2). – **IR** (ATR) $\tilde{\nu}$ [cm^{-1}] = 3372 (w, ν(NH)), 3005 (vw), 2922 (0.85), 2851 (vw), 1591 (w), 1563 (w), 1492 (m), 1433 (w), 1305 (w), 1280 (w), 1239 (w), 1173 (w), 1151 (w), 1108 (w), 1091 (w), 1027 (vw), 996 (vw), 977 (vw), 938 (vw), 886 (w), 800 (w), 780 (vw), 741 (m), 716 (w), 693 (m), 659 (w), 642 (w), 615 (vw), 588 (vw).). – **MS** (EI, 70 eV) *m/z* [%] = 300 (17) $[M+H]^+$, 299 (73) $[M]^+$, 298 (34) $[M–H]^+$, 195 (78) $[M–C_8H_8]^+$, 194 (84) $[M–C_8H_9]^+$, 193 (24) $[M–C_8H_{10}]^+$, 104 (100) $[C_8H_8]^+$. – **HRMS** ($C_{22}H_{21}N$) calc. 299.1669; found 299.1670. – **HRMS** (APCI, $C_{22}H_{21}N$) calc. 300.1747 $[M+H]^+$; found 300.1737 $[M+H]^+$. Analytical data matches that of the literature.[4]

rac-4-N-(Phenyl)amino[2.2]paracyclophane 1 H

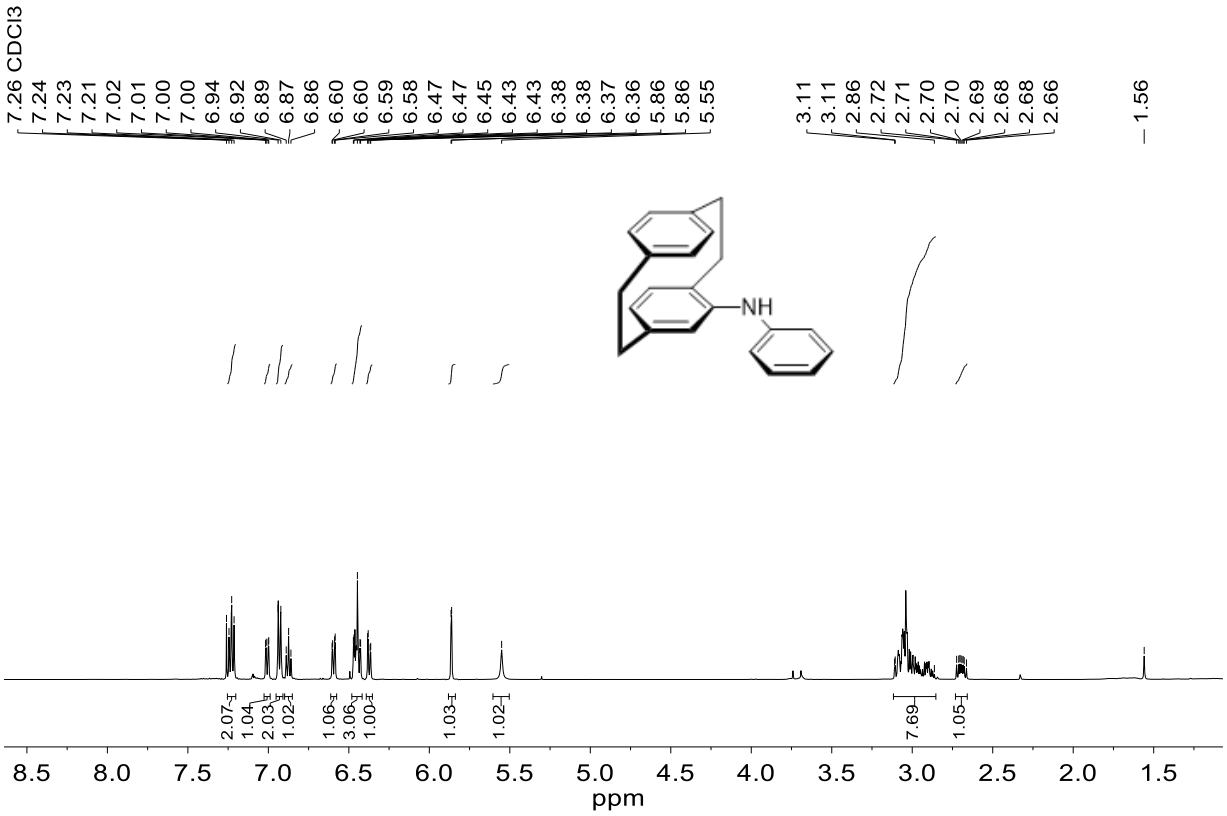

rac-4-N-(Phenyl)amino[2.2]paracyclophane 13 C

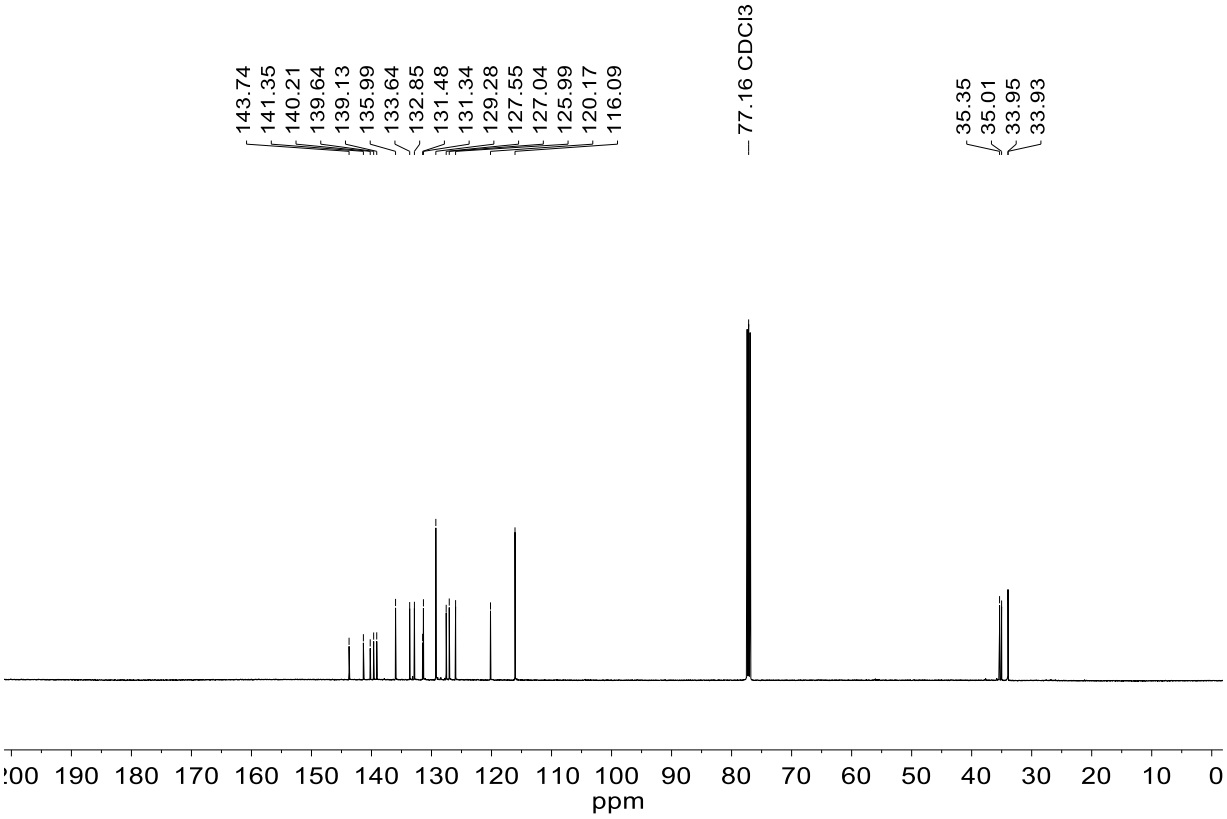

***rac*-[2]Paracyclo[2](1,4)carbazolophane (Carbazolophane)**

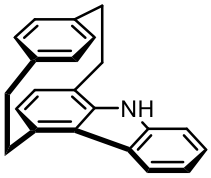

In a 25 mL three neck flask equipped with a reflux condenser, 1.50 g of *rac*-4-*N*-(phenyl)amino[2.2]paracyclophane (5.00 mmol, 1.00 equiv.), 225 mg of palladium acetate (1.00 mmol, 20 mol%) and 306 mg of pivalic acid (3.00 mmol, 60 mol%) were dissolved in 25 mL of acetic acid and the mixture was stirred at 120 °C for 7 h. While stirring, compressed air was added continuously to the suspension using a Teflon hose. The crude product was dissolved in 100 mL of water and 50 mL of ethyl acetate. Then, the mixture was neutralized by adding solid potassium hydroxide and solid sodium bicarbonate and extracted with 50 mL of ethyl acetate three times. The combined organic layers were washed with 50 mL of brine and dried over Na_2SO_4. The dark brown filtrate was evaporated under reduced pressure and the residue was purified by flash chromatography (silica, 10:1 cyclohexane:ethyl acetate) to yield 560 mg (38%, 1.88 mmol) of a white solid. – $\mathbf{R_f}$ = 0.29 (cyclohexane:ethyl acetate 10:1) – **^{1}H NMR** (400 MHz, $CDCl_3$) δ [ppm] = 8.06 (d, $^3J_{HH}$ = 7.9 Hz, 1H), 7.90 (br s, 1H), 7.46 (d, $^3J_{HH}$ = 8.2 Hz, 1H), 7.40 (t, $^3J_{HH}$ = 7.5 Hz, 1H), 7.29 – 7.23 (m, 1H), 6.63 (d, $^3J_{HH}$ = 7.5 Hz, 1H), 6.56 (d, $^3J_{HH}$ = 7.5 Hz, 1H), 6.50 (dd, $^3J_{HH}$ = 7.8 Hz, $^4J_{HH}$ = 1.9 Hz, 1H), 6.36 (dd, $^3J_{HH}$ = 7.8 Hz, $^4J_{HH}$ = 2.0 Hz, 1H), 5.94 (dd, $^3J_{HH}$ = 7.7 Hz, $^4J_{HH}$ = 2.0 Hz, 1H), 5.22 (dd, $^3J_{HH}$ = 7.7 Hz, $^4J_{HH}$ = 1.9 Hz, 1H), 4.03 –3.98 (m, 1H), 3.42 – 3.27 (m, 1H), 3.18 – 2.87 (m, 6H). – **^{13}C NMR** (101 MHz, $CDCl_3$) δ [ppm] = 140.14 (C_{quat}, C_{Ar}), 138.94 (C_{quat}, C_{Ar}), 138.01 (C_{quat}, C_{Ar}), 137.41 (C_{quat}, C_{Ar}), 135.89 (C_{quat}, C_{Ar}), 132.12 (+, $C_{Ar}H$), 131.60 (+, $C_{Ar}H$), 131.09 (+, $C_{Ar}H$), 126.57 (+, $C_{Ar}H$), 126.41 (+, $C_{Ar}H$), 125.52 (C_{quat}, C_{Ar}), 125.35 (C_{quat}, C_{Ar}), 124.97 (+, $C_{Ar}H$), 124.67 (+, $C_{Ar}H$), 122.53 (+, $C_{Ar}H$), 122.31 (C_{quat}, C_{Ar}), 119.78 (+, $C_{Ar}H$), 110.76 (+, $C_{Ar}H$), 34.05 (–, CH_2), 33.86 (–, CH_2), 33.35 (–, CH_2), 31.22 (–, CH_2). – **IR** (ATR) $\tilde{\nu}$ [cm^{-1}] = 3389 (w, ν(NH)), 3031 (vw), 3005 (vw), 2986 (vw), 2923 (w), 2581 (vw), 1592 (vw), 1499 (w), 1455 (w), 1436 (w), 1393 (w), 1321 (w), 1298 (w), 1246 (w), 1026 (w), 931 (w), 871 (w), 805 (w), 770 (vw), 749 (m), 735 (m), 719 (w), 671 (w), 609 (w), 585 (w), 569 (vw), 514 (w), 470 (w) . – **HRMS** (APCI, $C_{22}H_{19}N$) calc. 298.1590 $[M+H]^+$; found 298.1581 $[M+H]^+$. Analytical data matches that of the literature.[4]

rac-[2]Paracyclo[2](1,4)carbazolophane 1 H

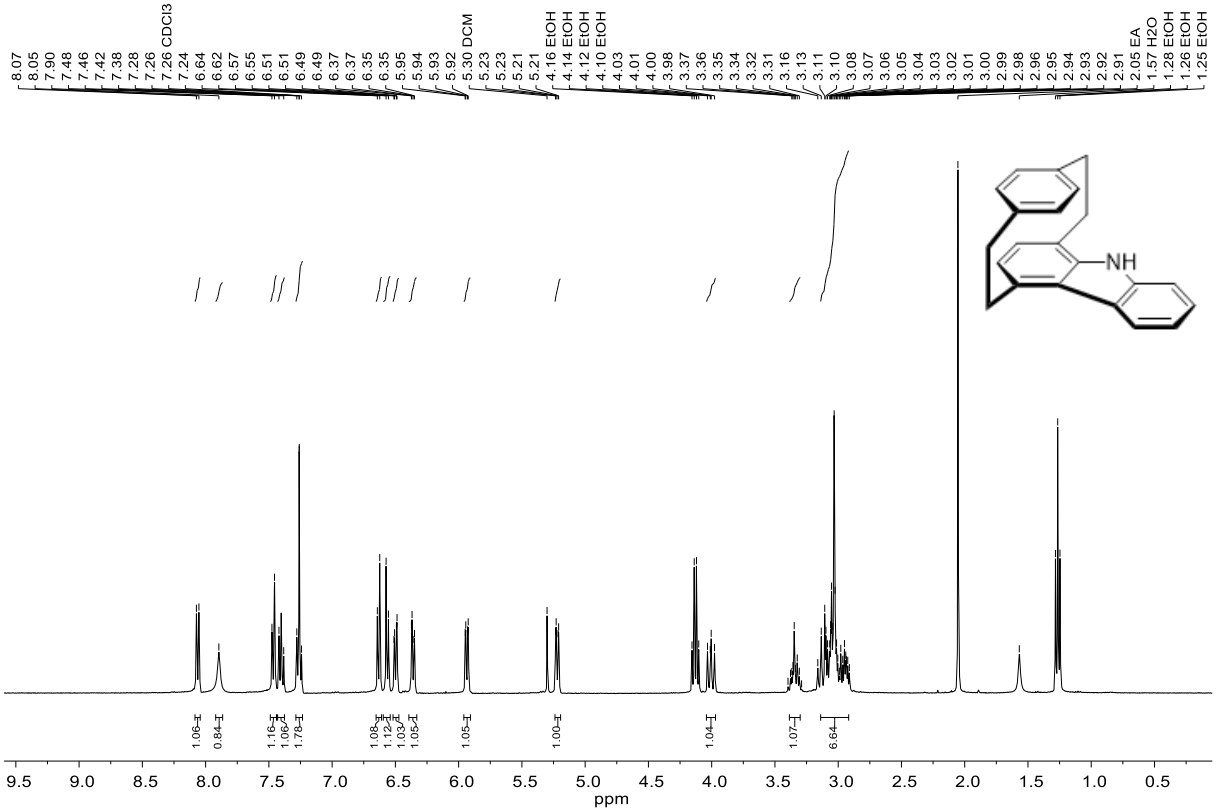

rac-[2]Paracyclo[2](1,4)carbazolophane 13 C

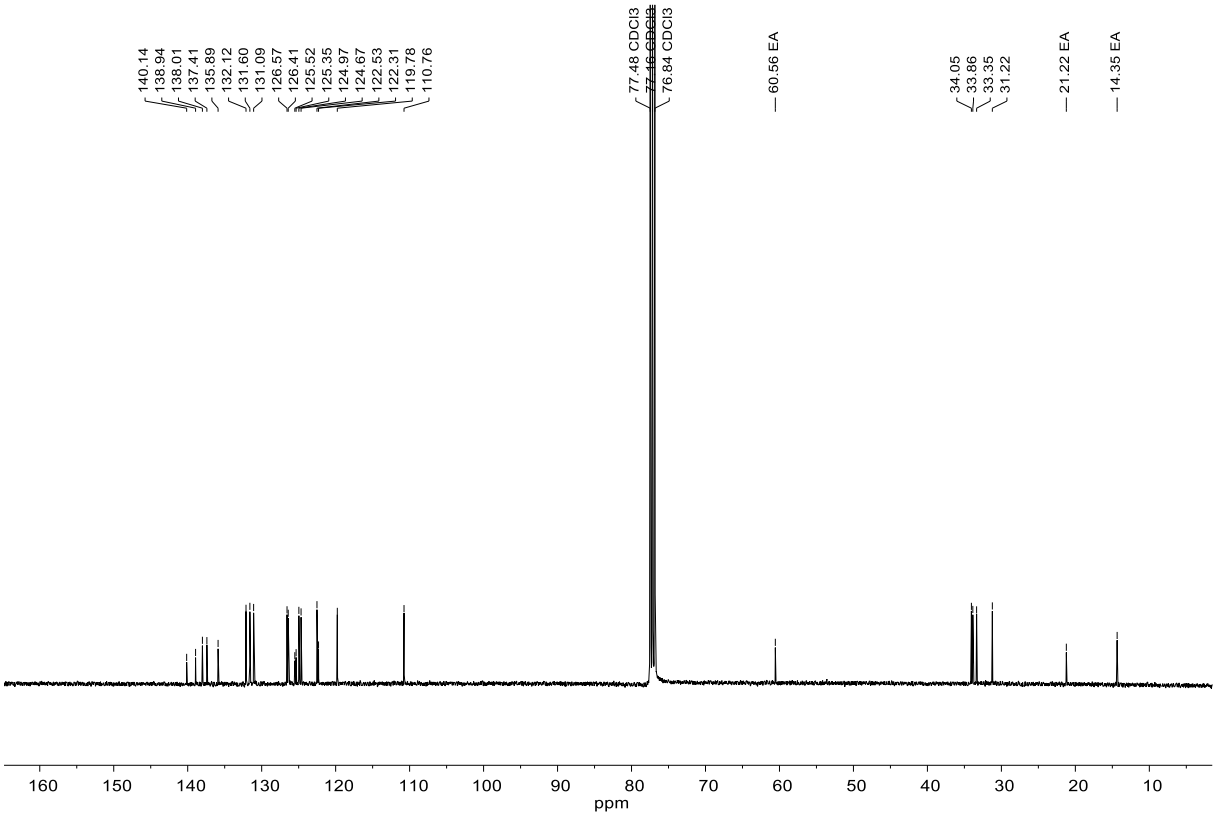

2-(4-Fluorophenyl)-4,6-diphenyl-1,3,5-triazine

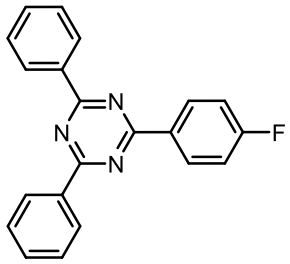

In a 250 mL Schlenk flask equipped with a reflux condenser 5.18 g of 2-chlorophenyl-4,6-diphenyl-1,3,5-triazine (19.3 mmol, 1.00 equiv.), 4.06 g of (4-fluorophenyl)boronic acid (29.0 mmol, 1.50 equiv.), 5.34 g of potassium carbonate (38.7 mmol, 2.00 equiv.) and 1.50 g of $Pd(PPh_3)_4$ (1.30 mmol, 7 mol%) were dissolved in 150 mL of dry toluene under argon atmosphere. 0.50 mL of water was then added to the reaction mixture. The yellowish reaction mixture was stirred at 75 °C for 19 h. Then, the mixture was diluted with 100 mL of water and 100 mL of ethyl acetate. After extraction, the organic layer was washed with 100 mL of brine three times and dried over Na_2SO_4. The yellow filtrate was evaporated under reduced pressure, and the brown crude product was purified by flash chromatography (silica, 2:1 cyclohexane:ethyl acetate) to yield 5.23 g (83%, 16.0 mmol) of a white fibrous solid. – $\mathbf{R_f}$ = 0.50 (CH/DCM 50:1). – **^{1}H NMR** (500 MHz, $CDCl_3$) δ [ppm] = 8.83 – 8.71 (m, 6H), 7.66 – 7.54 (m, 6H), 7.25 (t, $^3J_{HH}$ = 8.6 Hz, 2H). – **^{13}C NMR** (125 MHz, $CDCl_3$) δ [ppm] = 171.75, 170.76, 165.93 (C_{quat}, d, $^1J_{CF}$ = 253.0 Hz), 136.23 (C_{quat}, C_{Ar}), 132.73 (+, C_{Ar}), 132.52 (C_{quat}, d, $^4J_{CF}$ = 2.9 Hz, C_{Ar}), 131.43 (+, d, $^3J_{CF}$ = 9.0 Hz, $C_{Ar}H$), 129.08 (+, C_{Ar}), 128.79 (+, C_{Ar}), 115.84 (+, d, $^2J_{CF}$ = 21.8 Hz, $C_{Ar}H$). – **^{19}F NMR** (470 MHz, $CDCl_3$) δ [ppm] = –107.1 (1F). – **IR** (ATR) $\tilde{\nu}$ [cm^{-1}] = 3055 (w), 1915 (w), 1601 (m), 1509 (s), 1446 (m), 1412 (m), 1362 (s), 1224 (m), 1175 (m), 1142 (m), 1066 (m), 1026 (m), 855 (m), 832 (m), 764 (s), 728 (m), 685 (s), 644 (m), 583 (m), 503 (m), 469 (w), 392 (w).– **EA** ($C_{21}H_{14}FN_3$) calc. N: 12.84, C:77.05, H: 4.31; found N: 12.80, C: 76.95, H: 4.31. – **HRMS** (APCI, $C_{21}H_{14}FN_3$) calc. 328.1245 $[M+H]^+$; found 328.1234 $[M+H]^+$. Analytical data matches that of the literature.[6]

2-(4-Fluorophenyl)-4,6-diphenyl-1,3,5-triazine 19 F

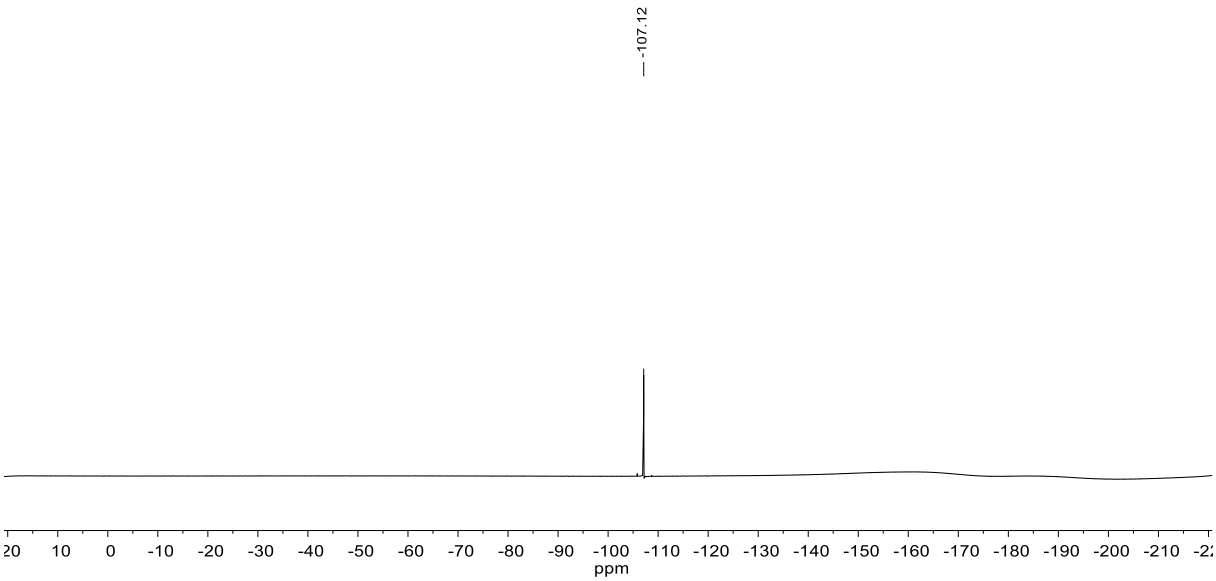

2-(4-Fluorophenyl)-4,6-diphenyl-1,3,5-triazine 1 H

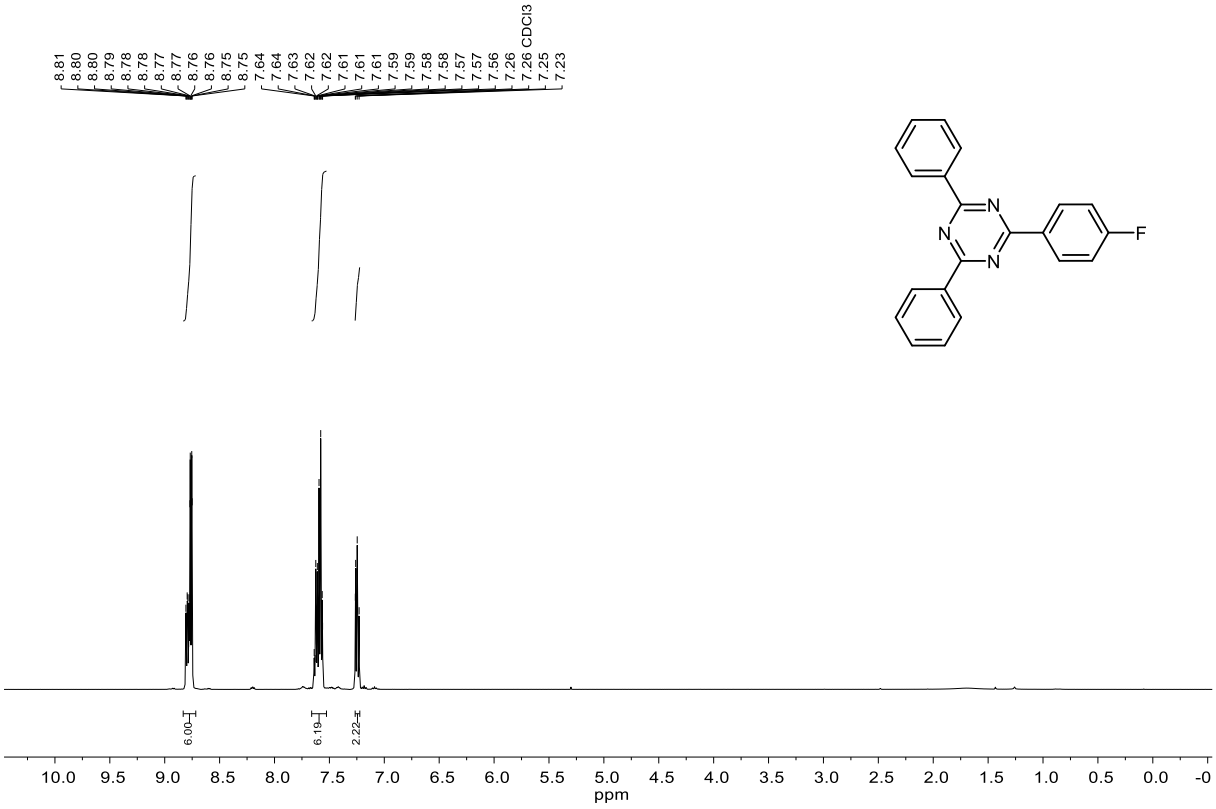

2-(4-Fluorophenyl)-4,6-diphenyl-1,3,5-triazine 13 C

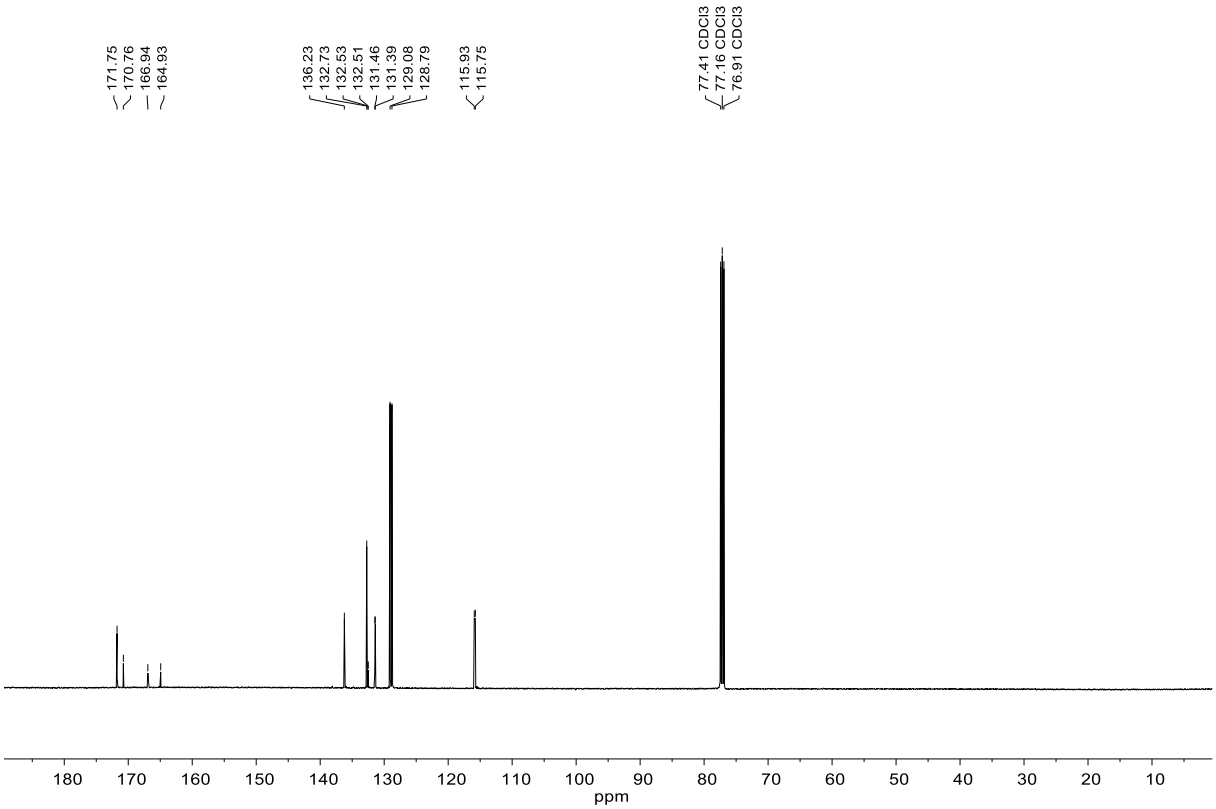

9-(4-(4,6-Diphenyl-1,3,5-triazin-2-yl)phenyl)-9*N*-carbazole

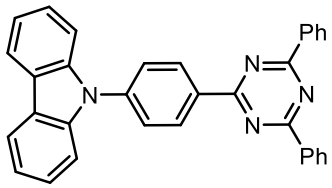

In a pressure vial, 92.0 mg of carbazole (550 µmol, 1.00 equiv.), 360 mg of the fluoride 2-(4-fluorophenyl)-4,6-diphenyl-1,3,5-triazine (1.10 mmol, 2.00 equiv.) and 257 mg of tripotassium phosphate (1.21 mmol, 2.20 equiv.) were dissolved in 8 mL of DMSO and stirred at 115 °C for 16 h. After cooling to room temperature, the mixture was diluted with 30 mL ethyl acetate and washed with 50 mL of brine three times. The organic layer was dried over Na_2SO_4. Afterwards, the solvent was evaporated under reduced pressure and the residue was purified by flash chromatography (silica, 50:1, 10:1, 5:1, 2:1 gradient cyclohexane:DCM) to yield 52.1 mg (42%, 110 µmol) of a yellow solid that luminesced. – **R_f** = 0.28 (cyclohexane/DCM 10:1). – **Mp** = 270 °C. – **^{1}H NMR** (500 MHz, $CDCl_3$) δ [ppm] = 9.03 (d, $^3J_{HH}$ = 8.6 Hz, 2H), 8.83 (d, $^3J_{HH}$ = 8.2 Hz, 4H), 8.18 (d, $^3J_{HH}$ = 7.8 Hz, 2H), 7.83 (d, $^3J_{HH}$ = 8.5 Hz, 2H), 7.69 – 7.59 (m, 6H), 7.57 (d, $^3J_{HH}$ = 8.2 Hz, 2H), 7.46 (t, $^3J_{HH}$ = 7.7 Hz, 2H), 7.34 (t, $^3J_{HH}$ = 7.5 Hz, 2H). – **^{13}C NMR** (126 MHz, $CDCl_3$) δ [ppm] = 171.95(C_{quat}, C_{Ar}), 171.08 (C_{quat}, C_{Ar}), 141.75 (C_{quat}, C_{Ar}), 140.57 (C_{quat}, C_{Ar}), 136.27 (C_{quat}, C_{Ar}), 135.09 (C_{quat}, C_{Ar}), 132.82(+, $C_{Ar}H$), 130.79 (+, $C_{Ar}H$), 129.16 (+, $C_{Ar}H$), 128.87(+, $C_{Ar}H$), 126.88 (+, $C_{Ar}H$), 126.30 (+, $C_{Ar}H$), 123.89 (C_{quat}, C_{Ar}), 120.58 (+, $C_{Ar}H$), 120.55(+, $C_{Ar}H$), 110.07(+, $C_{Ar}H$). – **IR** (ATR) $\tilde{\nu}$ [cm^{-1}] = 3054 (vw), 2850 (vw), 2921 (w), 1589 (w), 1512 (m), 1444 (m), 1366 (m), 1223 (w), 1169 (w), 1026 (w), 827 (w), 765 (m), 737 (m), 720 (m), 686 (m), 647 (w), 621 (w), 562 (w), 505 (w), 466 (w), 418 (w). – **EA** ($C_{33}H_{22}N_4$) calc. C: 83.52, H: 4.67, N: 11.81; found C: 82.29, H: 4.56, N: 11.54. – **HRMS** (APCI, $C_{33}H_{22}N_4$) calc. 475.1917 $[M+H]^+$; found 475.1900 $[M+H]^+$. Analytical data matches that of the literature.[7]

9-(4-(4,6-Diphenyl-1,3,5-triazin-2-yl)phenyl)-9N-carbazole 1 H

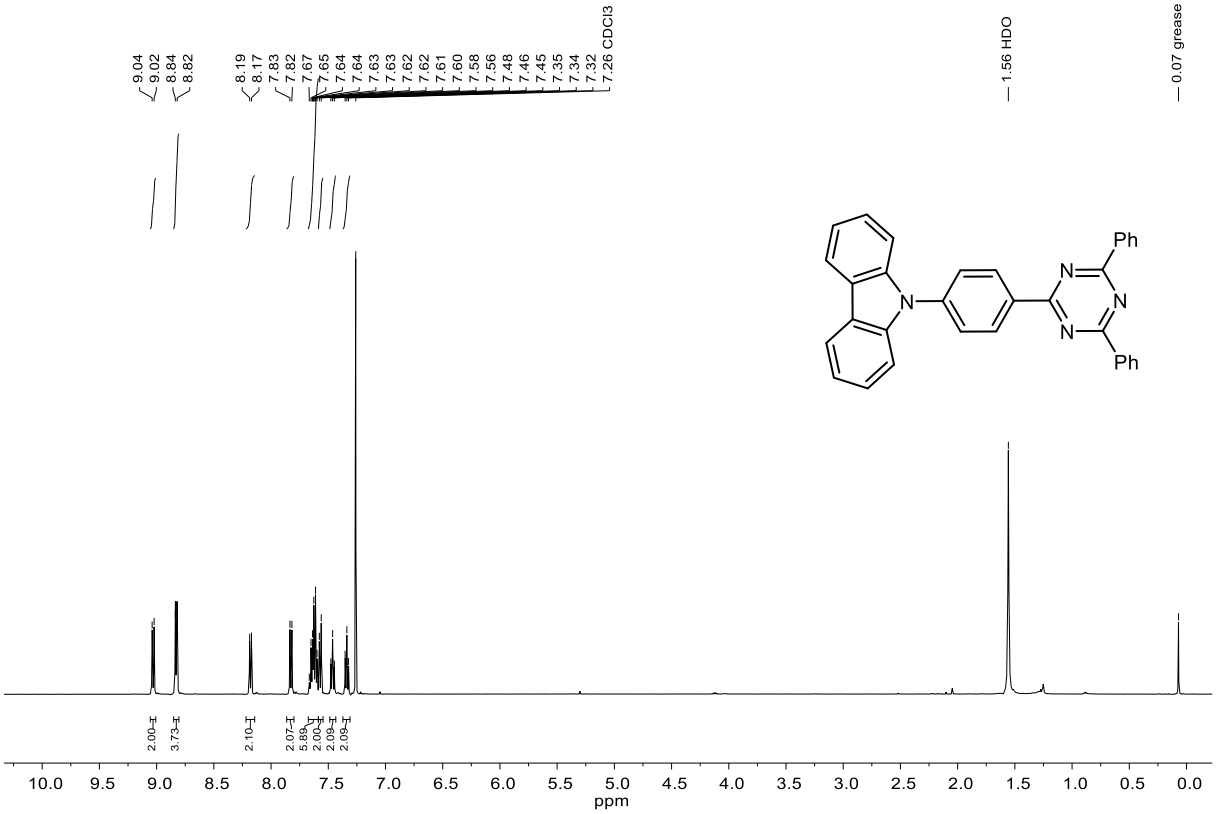

9-(4-(4,6-Diphenyl-1,3,5-triazin-2-yl)phenyl)-9N-carbazole 13 C

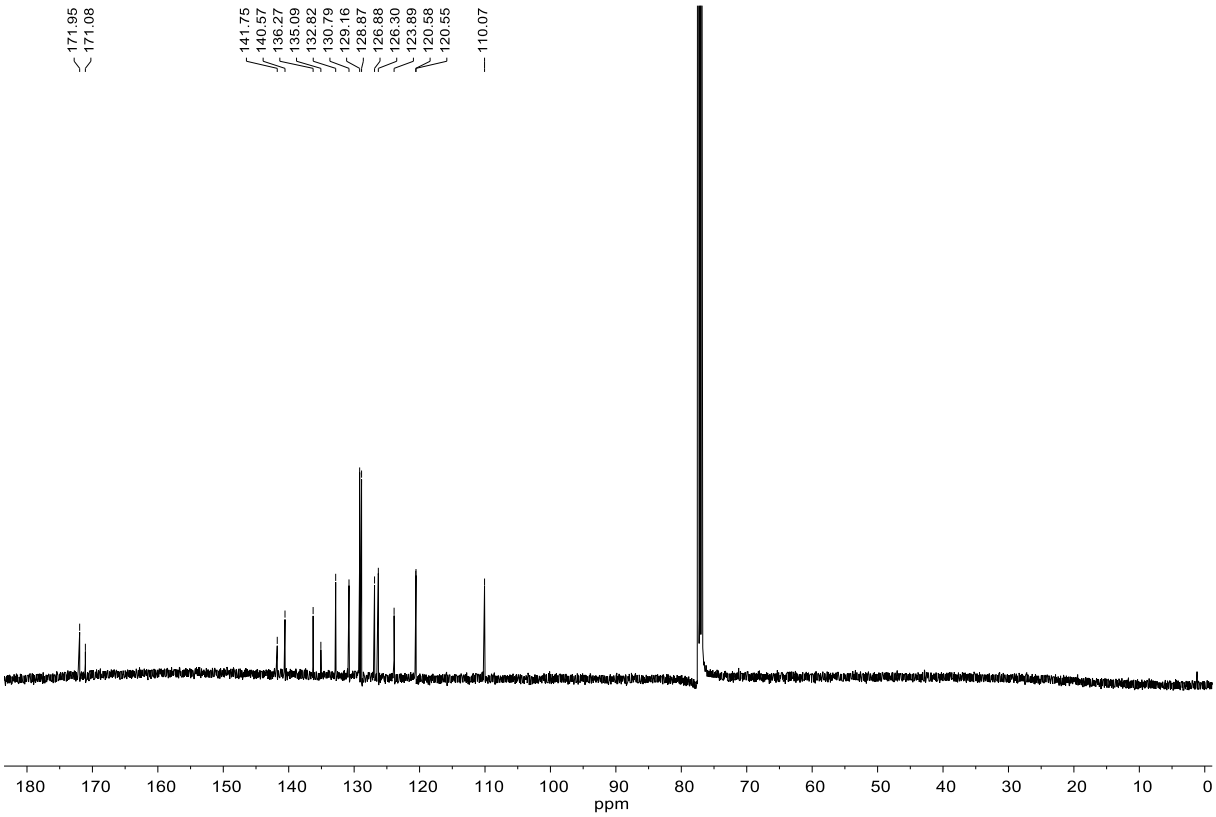

***rac*-1-(*N*-Carbazolophanyl)-4-(4,6-diphenyl-1,3,5-triazin-2-yl)-benzene**

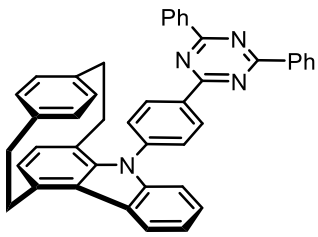

In a pressure vial, 125 mg of *rac*-[2]paracyclo[2](1,4)carbazolophane (420 µmol, 1.00 equiv.), 275 mg of 2-(4-fluorophenyl)-4,6-diphenyl-1,3,5-triazine (840 µmol, 2.00 equiv.) and 196 mg of tripotassium phosphate (924 µmol, 2.20 equiv.) were dissolved in 8 mL of DMSO and stirred at 115 °C for 16 h. After cooling to room temperature, the mixture was diluted with 30 mL of ethyl acetate and washed with 50 mL of brine three times. The organic layer was dried over Na_2SO_4. Afterwards, the solvent was evaporated under reduced pressure and the residue was purified by flash chromatography (silica, 100:1, 50:1, 10:1, 5:1, 1:1 gradient cyclohexane:DCM) to yield 215 mg (84%, 355 µmol) of a yellow and highly luminescent solid. – **R_f** = 0.28 (CH/DCM 10:1). – **Mp** = 263 °C. – **^{1}H NMR** (500 MHz, $CDCl_3$) δ [ppm] = 9.03 (bs, 2H), 8.88 – 8.81 (m, 4H), 8.17 (d, $^3J_{HH}$ = 7.8 Hz, 1H), 7.72 – 7.57 (m, 8H), 7.56 (d, $^3J_{HH}$ = 8.1 Hz, 1H), 7.42 (t, $^3J_{HH}$ = 7.6 Hz, 1H), 7.36 (t, $^3J_{HH}$ = 7.4 Hz, 1H), 6.73 – 6.64 (m, 2H), 6.51 (dd, $^3J_{HH}$ = 7.8, $^4J_{HH}$ = 1.8 Hz, 1H), 6.35 (dd, $^3J_{HH}$ = 7.8, $^4J_{HH}$ = 1.8 Hz, 1H), 5.98 (dd, $^3J_{HH}$ = 7.6, $^4J_{HH}$ = 1.8 Hz, 1H), 5.54 (dd, $^3J_{HH}$ = 7.7, $^4J_{HH}$ = 1.8 Hz, 1H), 4.11 – 4.05 (m, 1H), 3.26 – 3.03 (m, 3H), 2.94 – 2.85 (m, 1H), 2.84 – 2.66 (m, 2H), 2.29 (ddd, $^3J_{HH}$ = 13.1, 9.6, $^2J_{HH}$ = 7.3 Hz, 1H). – **^{13}C NMR** (125 MHz, $CDCl_3$) δ [ppm] = 171.95 (C_{quat}, C_{Ar}), 171.04 (C_{quat}, C_{Ar}), 142.88 (C_{quat}, C_{Ar}), 140.68 (C_{quat}, C_{Ar}), 140.56 (C_{quat}, C_{Ar}), 138.11 (C_{quat}, C_{Ar}), 137.56 (C_{quat}, C_{Ar}), 136.26 (C_{quat}, C_{Ar}), 135.94 (C_{quat}, C_{Ar}), 134.94 (C_{quat}, C_{Ar}), 133.67 (+, $C_{Ar}H$), 132.83 (+, $C_{Ar}H$), 131.76 (+, $C_{Ar}H$), 131.37 (+, $C_{Ar}H$), 130.31 (+, $C_{Ar}H$), 129.16 (+, $C_{Ar}H$), 129.09 (+, $C_{Ar}H$), 128.87 (+, $C_{Ar}H$), 128.80 (+, $C_{Ar}H$), 127.82 (+, $C_{Ar}H$), 127.13 (C_{quat}, C_{Ar}), 126.71 (+, $C_{Ar}H$), 125.88 (C_{quat}, C_{Ar}), 125.78 (+, $C_{Ar}H$), 125.35 (+, $C_{Ar}H$), 124.59 (C_{quat}, C_{Ar}), 122.69 (+, $C_{Ar}H$), 121.03 (+, $C_{Ar}H$), 109.91 (+, $C_{Ar}H$), 35.14 (–, CH_2), 33.96 (–, CH_2), 33.57 (–, CH_2), 33.26 (–, CH_2). – **IR** (ATR) $\tilde{\nu}$ [cm^{-1}] = 3030 (vw), 2927 (vw), 2852 (vw), 1587 (vw), 1510 (w), 1444 (w), 1395 (w), 1364 (w), 1173 (w), 1025 (w), 890 (vw), 831 (w), 765 (w), 739 (w), 686 (w), 639 (w), 597 (vw), 527 (vw), 511 (w), 482 (vw), 415 (vw). – **EA** ($C_{43}H_{32}N_4$) calc. C: 85.40, H: 5.33, N: 9.26; found C: 84.75, H: 5.24, N: 9.34. – **HRMS** (APCI, $C_{43}H_{32}N_4$) calc. 605.2700 $[M+H]^+$; found 605.2678 $[M+H]^+$.

rac-1-(N-Carbazolophanyl)-4-(4,6-diphenyl-1,3,5-triazin-2-yl)-benzene 1 H

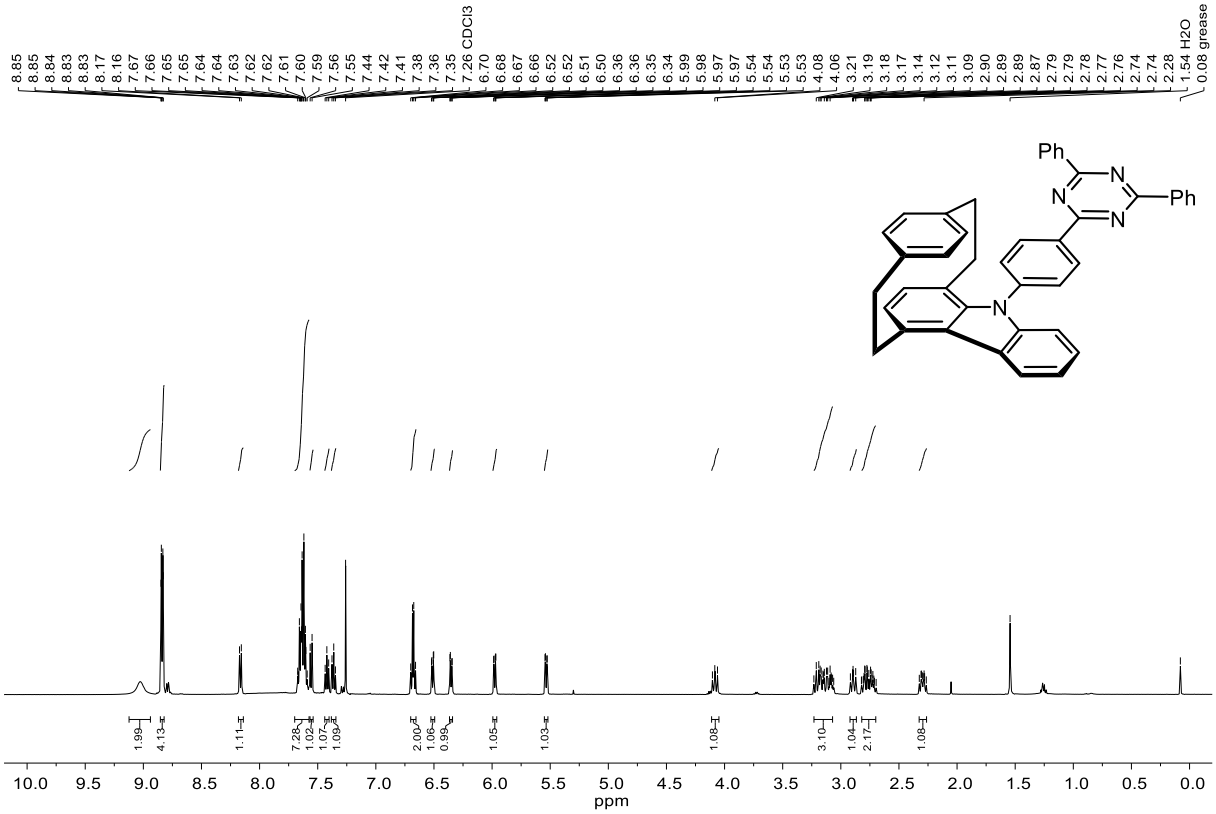

rac-1-(N-Carbazolophanyl)-4-(4,6-diphenyl-1,3,5-triazin-2-yl)-benzene 13 C

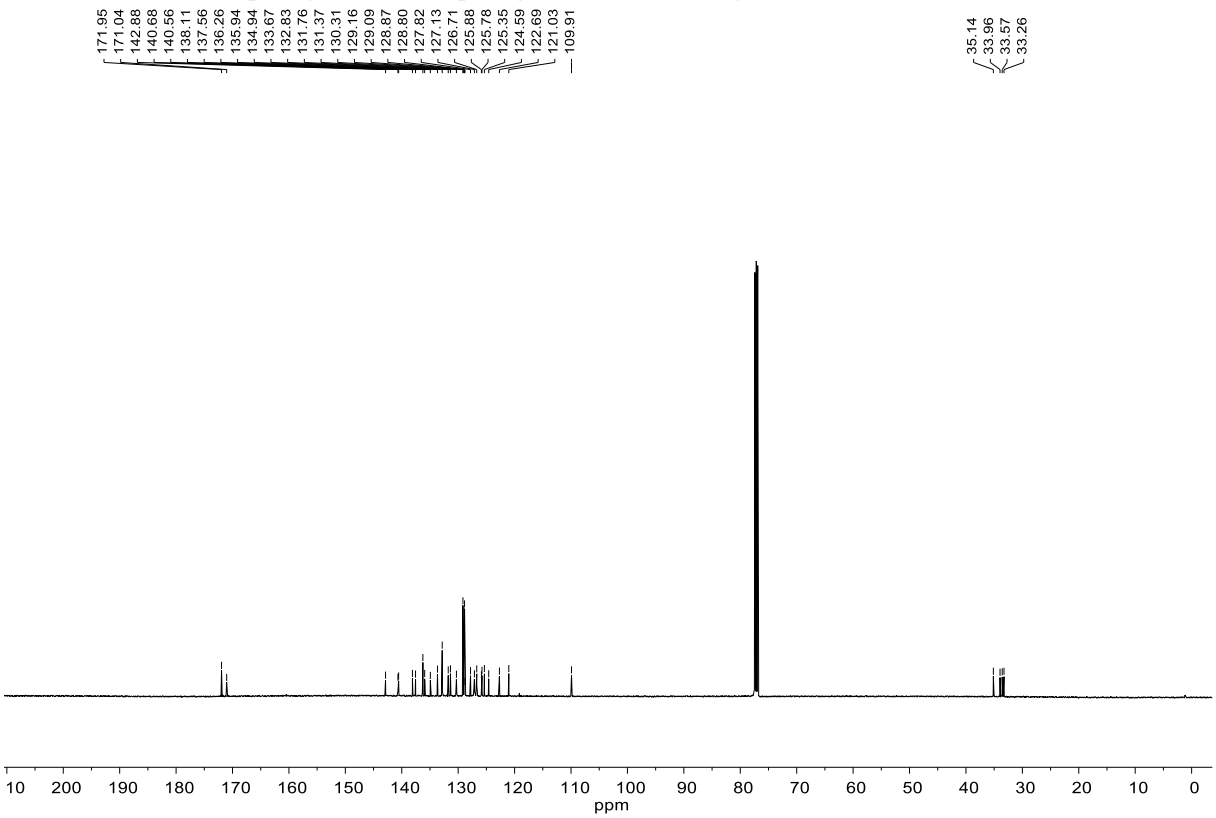

5. Chiral Separation and Determination of Alsolute Configuration

An overview of the strategy is shown in **Scheme S2**.

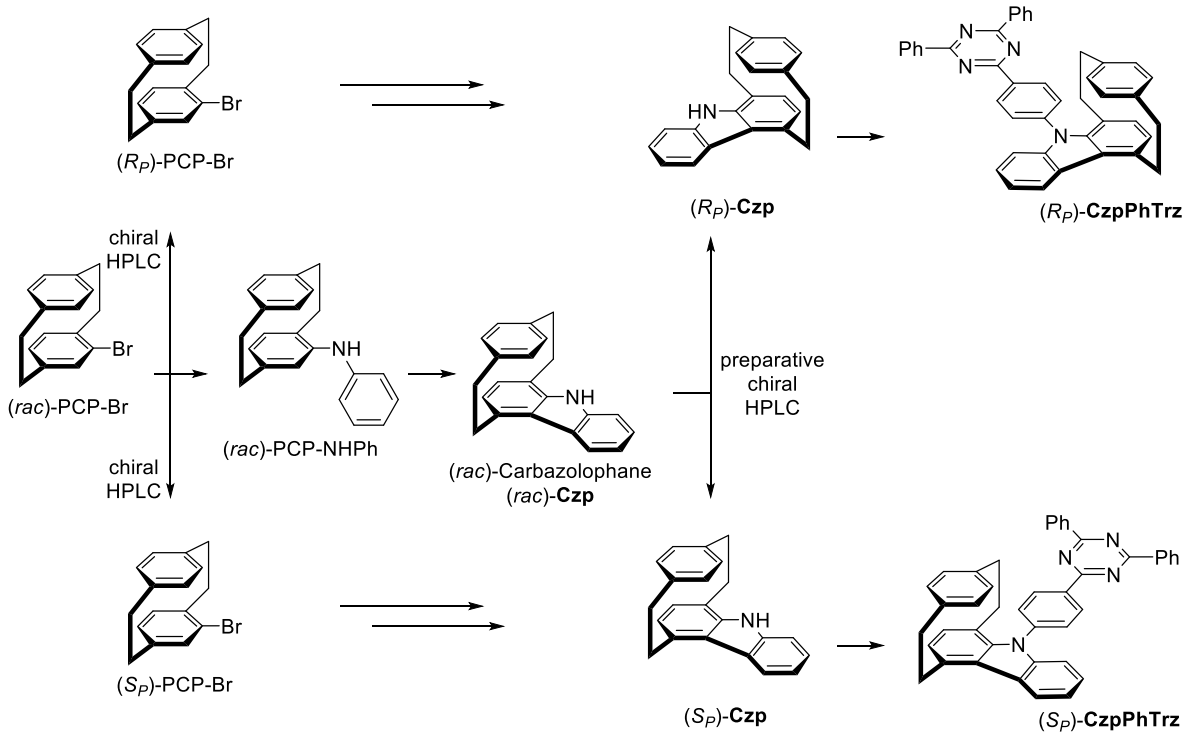

Scheme **S2**. Synthetic approach to the chiral emitters and the determination of absolute configuration.

Since the final emitter **CzpPhTrz** is very unpolar, it was unsuitable for a racemate separation on a semipreparative scale, but the free carbazolophane (**Czp**) was fit. The analytical HPLC chromatogram is shown in Figure **S4** to determine the enantiomeric excess, but it was also possible to separate the enantiomers on a semipreparative scale using the identical stationary phase.

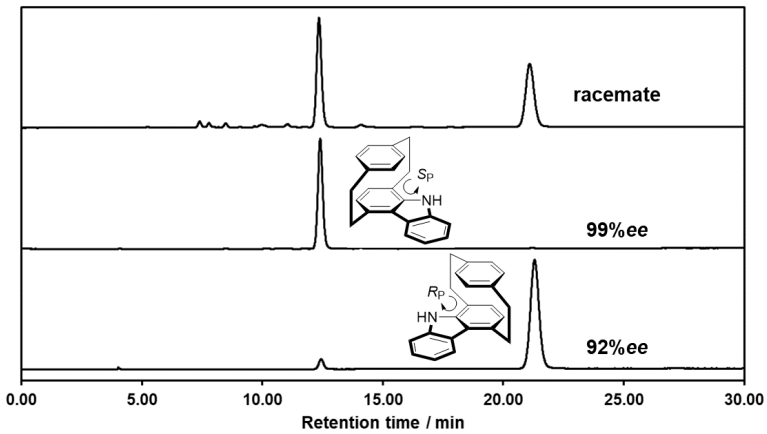

Figure **S4**. Analytical HPLC separation of **Czp**. A chiral Amylose-SA column from YMC was used as stationary phase with 10% isopropanol in n-hexane as the eluent with a 1.0 mL/min flow rate and detection at 256 nm.

To determine the absolute configuration (result already shown in **Figure S4**), the literature known bromide **PCP-Br** was separated into its enantiomers via semipreparative chiral HPLC using chiralpak-AZ (20 ×

250 mm, 5 µm) as the stationary phase and acetonitrile as the eluent (25 mL/min, 25 °C, 100 mg racemate loading per run). The absolute configurations for the first eluent (t_R 7.2 min) and second eluent (t_R 8.4 min) were determined by comparison of the circular dichroism (CD) spectra (Figure **S5**) with literature-known experimental and calculated data,[9] as well as with theory.[10]

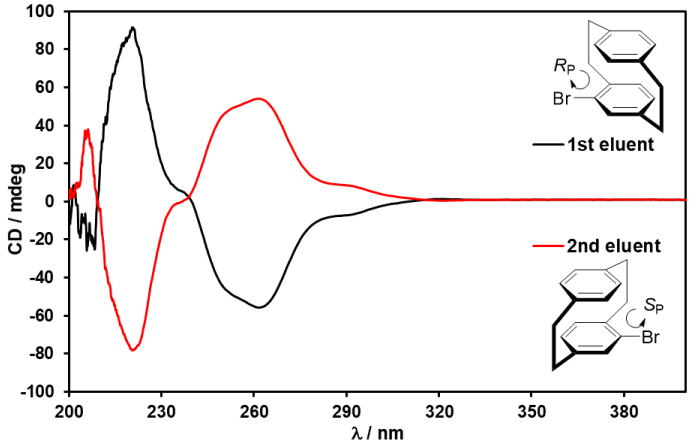

Figure **S5**. CD measurements in acetonitrile of 4-bromo[2.2]paracyclophane.

The final conversion to the respective enantioenriched emitter was then conducted with subsequent fractional recrystallization in order to increase the enantiomeric excess (Figure **S6**). Comparing the enantiomeric excess of (R_P)-emitter (93%ee) with the (R_P)-carbazolophane precursor (92%*ee*), the recrystallization did not serve to increase the *ee* in a significant manner. As the final emitter does not present pH-active groups, analytical HPLC runs had to be performed with a significantly reduced flow rate of 0.2 mL/min in order to observe a separation of the enantiomers.

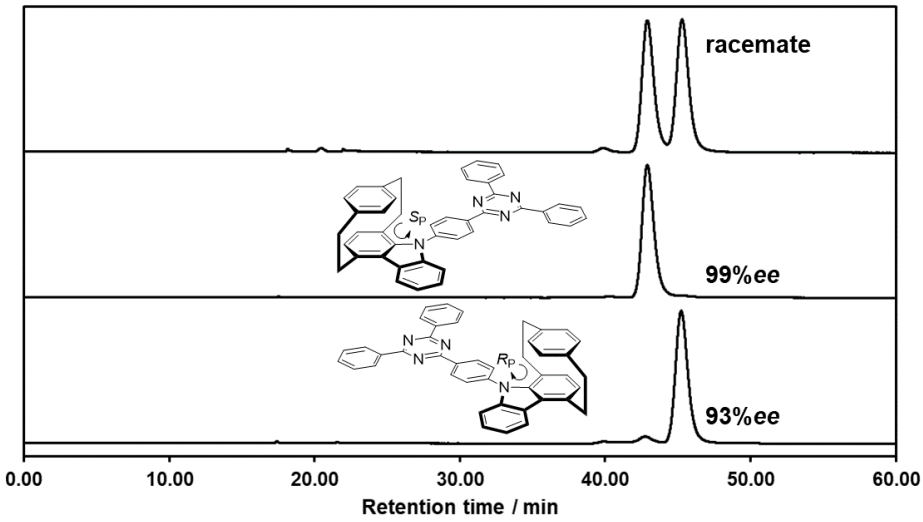

Figure **S6**. Analytical HPLC of **CzpPhTrz** emitters. Amylose-SA was used as the stationary phase with 2% isopropanol in n-hexane as the eluent with a 0.2 mL/min flow rate and detection at 256 nm. Top: Racemate for comparison. Middle: (S_P) with a determined enantiomeric excess of 99%. Bottom: (R_P) with a determined enantiomeric excess of 93%.

6. Crystallography

Single crystal X-ray diffraction data were collected on a STOE STADI VARI diffractometer with monochromated Cu Kα (1.54186 Å) or Ga Kα (1.34143 Å) radiation at low temperature. Using Olex2,[11] the structures were solved with the ShelXS[12] structure solution program using Direct Methods and refined with the ShelXL[13] refinement package using Least Squares minimization. Refinement was performed with anisotropic temperature factors for all non-hydrogen atoms; hydrogen atoms were calculated on idealized positions. Crystallographic data for compounds **CzPhTrz** (CCDC 1871934) and **CzpPhTrz** (CCDC 1871935) have been deposited with the Cambridge Crystallographic Data Centre.

Table **S1**. Crystal data and structure refinement information for **CzPhTrz** and **CzpPhTrz**.

Compound	**CzPhTrz**	**CzpPhTrz**
	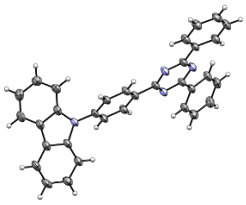	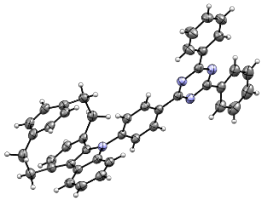
Empirical formula	$C_{33}H_{22}N_4$	$C_{43}H_{32}N_4$
Formula weight	474.54	604.72
Temperature/K	160.2	180.2
Crystal system	triclinic	monoclinic
Space group	$P\bar{1}$	$P2_1/c$
a/Å	3.8653(2)	15.6193(6)
b/Å	15.5368(8)	13.7087(4)
c/Å	19.5050(12)	14.6312(5)
α/°	101.550(4)	90
β/°	91.474(5)	94.394(3)
γ/°	94.709(4)	90
Volume/Å^3	1142.70(11)	3123.63(19)
Z	2	4
ρ_{calc}/g cm^{-3}	1.379	1.286
μ/mm^{-1}	0.413	0.586
F(000)	496.0	1272.0
Crystal size/mm^3	0.22 × 0.04 × 0.03	0.34 × 0.28 × 0.02
Radiation	GaKα (λ = 1.34143)	CuKα (λ = 1.54186)
2Θ range for data collection/°	5.07 to 113.9	12.13 to 128.0
Index ranges	$-1 \le h \le 4$, $-19 \le k \le 19$, $-24 \le l \le 24$	$-17 \le h \le 18$, $-15 \le k \le 13$, $-17 \le l \le 14$
Reflections collected	13397	14283
Independent reflections	4564 [R_{int} = 0.0509, R_σ = 0.0386]	5057 [R_{int} = 0.0604, R_σ = 0.0492]
Indep. refl. with I ≥ 2σ(I)	3112	3700
Data/restraints/parameters	4564/0/334	5057/0/425
Goodness-of-fit on F^2	0.922	1.035
Final R indexes [I ≥ 2σ(I)]	R_1 = 0.0470, wR_2 = 0.1193	R_1 = 0.0547, wR_2 = 0.1415
Final R indexes [all data]	R_1 = 0.0682, wR_2 = 0.1287	R_1 = 0.0872, wR_2 = 0.1569
Largest diff. peak/hole / e Å^{-3}	0.19/–0.29	0.22/–0.22
CCDC number	1871934	1871935

7. Electrochemical Characterization.

Electrochemistry measurements. Cyclic Voltammetry (CV) analysis was performed on an Electrochemical Analyzer potentiostat model 600D from CH Instruments. Samples were prepared as DCM solutions, which were degassed by sparging with DCM-saturated nitrogen gas for 10 minutes prior to measurements. All measurements were performed in 0.1 M DCM solution of tetrabutylammonium hexafluorophosphate, which was used as the supporting electrolyte. An Ag/Ag^+ electrode was used as the reference electrode while a glassy carbon electrode and a platinum wire were used as the working electrode and counter electrode, respectively. The redox potentials are reported relative to a saturated calomel electrode (SCE) with a ferrocene/ferrocenium (Fc/Fc^+) redox couple as the internal standard (0.46 V vs SCE).[14]

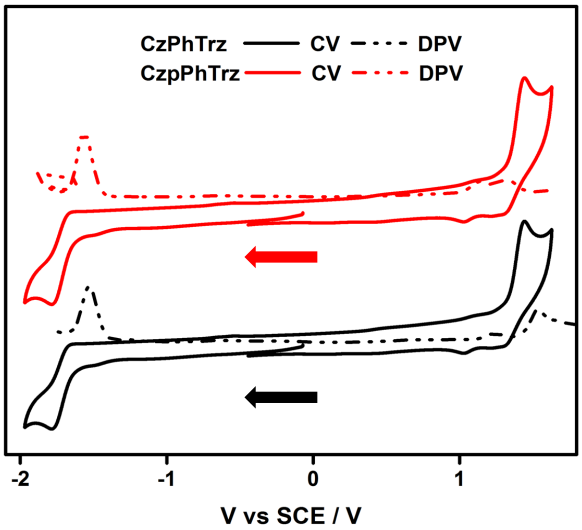

Figure **S7**. Cyclic Voltammograms and Differential Pulse Voltammograms of **CzPhTrz** and **CzpPhTrz** in degassed DCM (scan rate 100 mV s^{-1}).

8. Thermal Analysis.

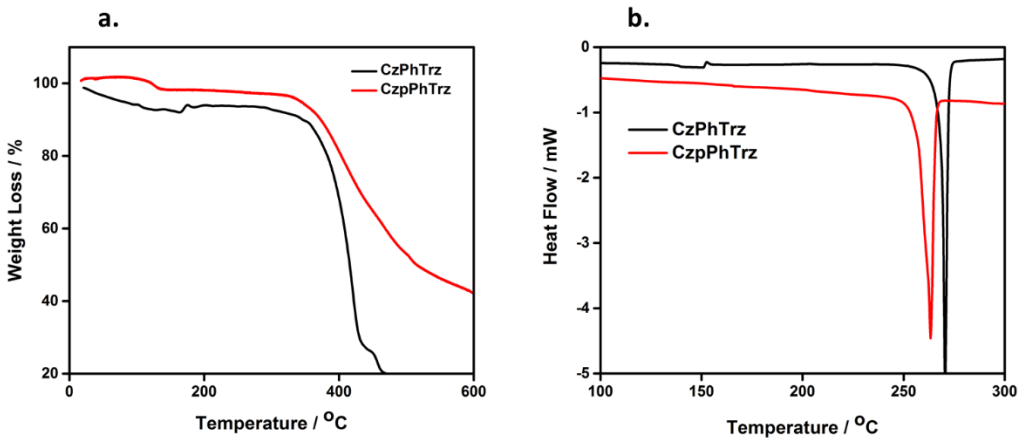

Figure **S8**. a.) TGA and b.) DSC measurements of **CzPhTrz** and **CzpPhTrz**.

9. Photophysical Characterization.

Photophysical measurements. Optically dilute solutions of concentrations on the order of 10^{-5} or 10^{-6} M were prepared in HPLC grade solvent for absorption and emission analysis. Absorption spectra were recorded at room temperature on a Shimadzu UV-1800 double beam spectrophotometer. Aerated solutions were bubbled with compressed air for 5 minutes whereas degassed solutions were prepared via three freeze-pump-thaw cycles prior to emission analysis using an in-house adapted fluorescence cuvette, itself purchased from Starna. Steady-state emission and time-resolved emission spectra were recorded at 298 K using an Edinburgh Instruments FLS980 fluorimeter. Samples were excited at 360 nm for steady-state measurements and at 378 nm for time-resolved measurements. Photoluminescence quantum yields for solutions were determined using the optically dilute method[15] in which four sample solutions with absorbance of ca. 0.100, 0.080, 0.060 and 0.040 at 360 nm were used. Their emission intensities were compared with those of a reference, quinine sulfate, whose quantum yield (Φ_r) in 1 *N* H_2SO_4 was determined to be 54.6% using absolute method.[16] The quantum yield of the sample, Φ_{PL}, can be determined by the equation $\Phi_{PL} = \Phi_r(A_r/A_s)((I_s/I_r)(n_s/n_r)^2$, where A stands for the absorbance at the excitation wavelength (λ_{exc} = 360 nm), I is the integrated area under the corrected emission curve and n is the refractive index of the solvent with the subscripts "s" and "r" representing sample and reference respectively. An integrating sphere was employed for quantum yield measurements for thin film samples.[17] Doped thin films were prepared by mixing the sample (10 wt.%) and PMMA in $CHCl_3$ followed by spin-casting on a quartz substrate. The Φ_{PL} of the films were then measured in air and by purging the integrating sphere with N_2 gas flow. Time-resolved PL measurements of the thin films were carried out using the time-correlated single-photon counting technique. The samples were excited at 378 nm by a pulsed laser diode (Picoquant, model PLS 370) and were kept in a vacuum of < 10^{-4} mbar. The singlet-triplet splitting energy ΔE_{ST} was estimated by recording the prompt fluorescence spectra and phosphorescence emission at 77 K in 10 wt.% doped films in DPEPO. The films were excited by a Q-switched Nd:YAG laser emitting at 355 nm (Laser-export). Emission from the samples was focused onto a spectrograph (Chromex imaging, 250is spectrograph) and detected on a sensitive gated iCCD camera (Stanford Computer Optics, 4Picos) having subnanosecond resolution.

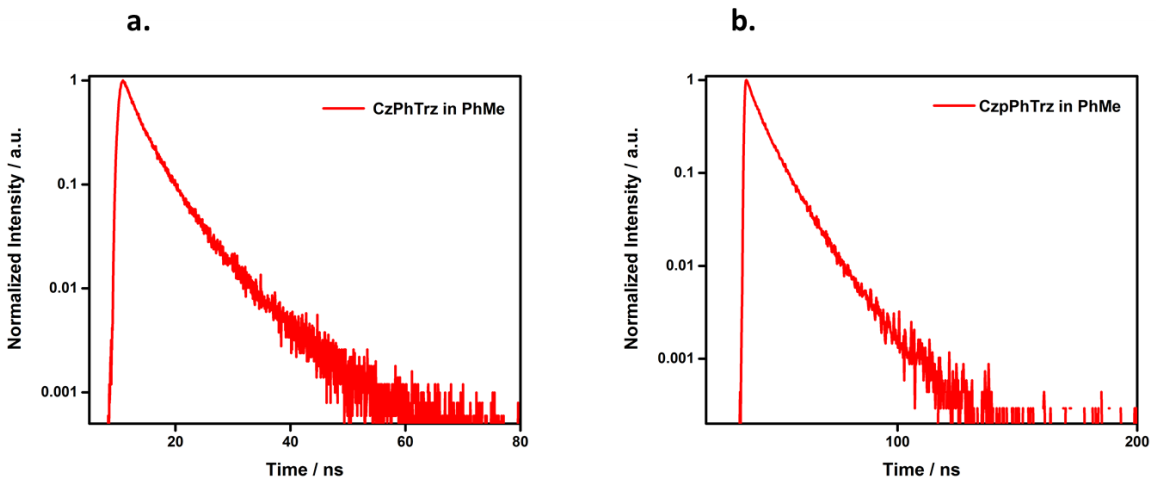

Figure **S9**. Transient PL decay curves of a.) **CzPhTrz** and b.) **CzpPhTrz** in degassed PhMe (λ_{exc} = 378 nm).

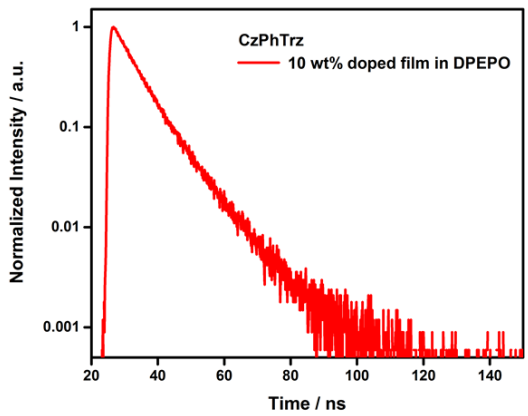

Figure **S10**. Time-resolved PL decay curve of **CzPhTrz** in 10 wt.% doped film in DPEPO (λ_{exc} = 378 nm).

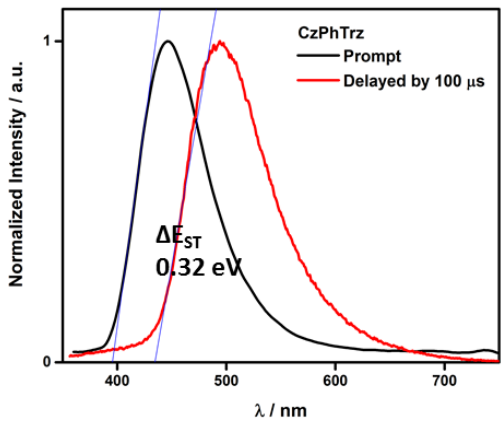

Figure **S11**. Prompt and delayed spectra (at 77K) of **CzPhTrz** in 10 wt.% doped film in DPEPO (λ_{exc} = 355 nm).

Table **S2**. Absolute Φ_{PL} measurements of doped films of **CzPhTrz** and **CzpPhTrz** in different host materials as a function of doping concentrations.

Host Material [a]	Φ^{b}_{PL} / %	
	CzPhTrz	**CzpPhTrz**
Neat Film	20	28
10 wt. % PMMA[c]	25	45
1 wt.% DPEPO	39	43
10 wt.% DPEPO[d]	50	69
7 wt.% PPT	-	62
15 wt.% mCP	48	65
10 wt.% CzSi	-	60

[a] Thin films were prepared by vacuum deposition and values were determined using an integrating sphere (λ_{exc} = 360 nm); degassing was done by N_2 purge. [b] Within error limit of +/- 2%. [c] Prepared by spin coating. [d] Average Φ_{PL} value of 5 different measurements.

10. DFT modelling

Computational methodology

DFT calculations were performed with the Gaussian 09 revision D.018 suite.[18] Initially the geometries of both emitters in the ground state in the gas phase were optimized employing the PBE0[19] functional with the standard Pople 6-31G(d,p) basis set.[20] Time-dependent DFT calculations were performed using the Tamm–Dancoff approximation (TDA).[21] The molecular orbitals were visualized using GaussView 5.0 software.

Table **S3.** Optimized atomic coordinates of compound **CzPhTrz** obtained from DFT calculations.

Center Number	Atomic Number	Atomic Type	Coordinates (Å) X	Y	Z
1	6	0	4.773569	-0.862680	0.732460
2	6	0	4.417040	-1.859427	1.638712
3	6	0	5.443086	-2.560657	2.259459
4	6	0	6.789580	-2.276506	1.994829
5	6	0	7.137384	-1.269447	1.105655
6	6	0	6.126249	-0.549447	0.468404
7	7	0	3.960676	-0.000119	-0.000095
8	6	0	4.773562	0.862550	-0.732544
9	6	0	6.126245	0.549440	-0.468354
10	6	0	4.417027	1.859274	-1.638811
11	6	0	7.137365	1.269565	-1.105483
12	6	0	5.443057	2.560636	-2.259431
13	6	0	6.789552	2.276616	-1.994662
14	1	0	8.180780	1.039180	-0.910700
15	1	0	5.192142	3.343626	-2.968680
16	1	0	7.565469	2.846334	-2.496194
17	6	0	2.555308	-0.000088	-0.000086
18	6	0	1.854024	-1.191682	-0.207762
19	6	0	1.854068	1.191534	0.207597
20	6	0	0.468611	-1.189587	-0.200125
21	1	0	2.405369	-2.107537	-0.392984
22	6	0	0.468659	1.189481	0.199997
23	1	0	2.405451	2.107375	0.392776
24	6	0	-0.239179	-0.000043	-0.000051
25	1	0	3.377652	2.074875	-1.861085
26	1	0	-0.088368	2.104991	0.364567
27	1	0	-0.088452	-2.105078	-0.364679
28	6	0	-1.713079	-0.000020	-0.000020
29	7	0	-2.334880	-1.163922	-0.210307
30	7	0	-2.334832	1.163906	0.210281
31	6	0	-3.670599	-1.112798	-0.203956
32	6	0	-3.670552	1.112827	0.203990
33	7	0	-4.381960	0.000027	0.000030
34	6	0	-4.408944	-2.368761	-0.437997
35	6	0	-5.807467	-2.375046	-0.427491
36	6	0	-3.715105	-3.560110	-0.673076
37	6	0	-6.500725	-3.557395	-0.649105

38	1	0	-6.330264	-1.443074	-0.243633
39	6	0	-4.411881	-4.740332	-0.894910
40	1	0	-2.631060	-3.538579	-0.678537
41	6	0	-5.805106	-4.741625	-0.883339
42	1	0	-7.586509	-3.557121	-0.639614
43	1	0	-3.868595	-5.662526	-1.077752
44	1	0	-6.348818	-5.665719	-1.057032
45	6	0	-4.408845	2.368820	0.438033
46	6	0	-5.807369	2.375137	0.427659
47	6	0	-3.714955	3.560165	0.672984
48	6	0	-6.500578	3.557513	0.649283
49	1	0	-6.330205	1.443170	0.243896
50	6	0	-4.411683	4.740415	0.894822
51	1	0	-2.630911	3.538609	0.678342
52	6	0	-5.804909	4.741739	0.883388
53	1	0	-7.586363	3.557263	0.639899
54	1	0	-3.868358	5.662607	1.077561
55	1	0	-6.348583	5.665855	1.057087
56	1	0	3.377673	-2.075154	1.860873
57	1	0	5.192175	-3.343655	2.968696
58	1	0	7.565503	-2.846112	2.496471
59	1	0	8.180791	-1.038962	0.910969

Table **S4.** Optimized atomic coordinates of compound **CzpPhTrz** obtained from DFT calculations.

Center Number	Atomic Number	Atomic Type	Coordinates (Å) X	Y	Z
1	6	0	3.440431	0.948624	0.275039
2	6	0	3.243274	1.822784	-0.806331
3	6	0	4.303074	2.698901	-1.039168
4	6	0	5.566582	2.518690	-0.468422
5	6	0	5.835094	1.434080	0.361440
6	6	0	4.719719	0.733967	0.845536
7	1	0	4.193762	3.436990	-1.830313
8	1	0	6.392686	3.126364	-0.828918
9	6	0	7.232130	0.872726	0.442006
10	1	0	7.553635	0.696496	1.474149
11	1	0	7.918424	1.620972	0.033435
12	6	0	2.199959	1.623781	-1.880737
13	6	0	7.403438	-0.473780	-0.374554
14	1	0	7.420793	-1.316893	0.322658
15	1	0	8.384298	-0.443938	-0.862018
16	6	0	2.358535	0.253398	-2.649211
17	1	0	1.634993	-0.464003	-2.248875
18	1	0	2.084884	0.428951	-3.695888
19	6	0	6.289233	-0.686461	-1.367634
20	6	0	6.111095	0.194410	-2.438341
21	6	0	4.856110	0.375390	-3.004807
22	1	0	6.926192	0.851480	-2.732659
23	6	0	3.991242	-1.391904	-1.655618
24	6	0	3.746315	-0.318458	-2.514099
25	1	0	4.711584	1.170602	-3.732519
26	1	0	3.160048	-2.003509	-1.313607
27	1	0	2.321985	2.441471	-2.598200
28	1	0	1.172271	1.686045	-1.510737
29	6	0	5.249362	-1.575920	-1.088996
30	7	0	2.560484	-0.007471	0.784653
31	6	0	3.248806	-0.821895	1.680999
32	6	0	4.595927	-0.398973	1.733471
33	6	0	2.770824	-1.863327	2.473613
34	6	0	5.485340	-1.071529	2.576599
35	6	0	3.678835	-2.516536	3.296520
36	6	0	5.024778	-2.131803	3.344186
37	1	0	6.523731	-0.765106	2.640309
38	1	0	3.333955	-3.338229	3.916839
39	1	0	5.711323	-2.662458	3.996380
40	1	0	5.376949	-2.322185	-0.309325
41	6	0	1.162725	-0.005576	0.636727
42	6	0	0.439343	1.177575	0.814729
43	6	0	0.489733	-1.189719	0.320700
44	6	0	-0.938266	1.174084	0.672754
45	1	0	0.972736	2.088822	1.065644

46	6	0	-0.890572	-1.190200	0.193654
47	1	0	1.060113	-2.098479	0.159525
48	6	0	-1.619027	-0.009261	0.365494
49	1	0	1.726000	-2.152483	2.455883
50	1	0	-1.424794	-2.100042	-0.055946
51	1	0	-1.512184	2.083609	0.810054
52	6	0	-3.085726	-0.009688	0.222618
53	7	0	-3.723869	1.155569	0.364986
54	7	0	-3.685104	-1.174756	-0.040237
55	6	0	-5.052375	1.105713	0.225890
56	6	0	-5.015218	-1.123104	-0.162987
57	7	0	-5.741607	-0.008090	-0.039397
58	6	0	-5.807776	2.364424	0.374905
59	6	0	-7.199479	2.370572	0.236412
60	6	0	-5.136717	3.558933	0.655770
61	6	0	-7.908422	3.556059	0.376767
62	1	0	-7.704633	1.436009	0.019372
63	6	0	-5.849179	4.742287	0.795890
64	1	0	-4.057683	3.537622	0.760074
65	6	0	-7.235473	4.743497	0.656648
66	1	0	-8.988813	3.555739	0.268229
67	1	0	-5.323586	5.667008	1.014199
68	1	0	-7.791549	5.670028	0.766472
69	6	0	-5.729643	-2.381287	-0.452564
70	6	0	-7.119832	-2.381231	-0.605373
71	6	0	-5.021948	-3.581341	-0.574996
72	6	0	-7.791177	-3.565651	-0.877553
73	1	0	-7.653745	-1.442650	-0.506961
74	6	0	-5.696903	-4.763908	-0.846453
75	1	0	-3.944655	-3.565033	-0.453118
76	6	0	-7.081865	-4.758688	-0.998453
77	1	0	-8.870543	-3.560148	-0.995693
78	1	0	-5.142950	-5.693111	-0.940018
79	1	0	-7.608390	-5.684633	-1.210880

---

11. Device Characterization.

OLED fabrication and characterization. The OLED devices were fabricated in bottom emitting architecture via vacuum sublimation in high vacuum at a base pressure of $2\text{-}5 \cdot 10^{-7}$ mbar. The organic layer sequence and the metal cathode were deposited onto pre-cleaned glass substrates coated with indium tin oxide (ITO) which has a sheet resistance of around 30 Ω/sq. A pre-patterned ITO glass substrate was treated by ultrasonic cleaning in acetone and isopropanol consecutively and then treated by oxygen plasma before the transfer to the vacuum chamber. Organic layers were deposited at a rate of 0.3-0.6 Å/s, which was controlled in situ using the quartz crystal monitors. Doping of the emission layers was achieved through co-evaporation of the emitter and host materials. The electron injection layer LiF was deposited at a rate of 0.10 Å/s while the Al cathode was deposited at a rate of 0.5 Å/s through the shadow mask defining the top electrode. The spatial overlap of the anode and cathode electrodes determined the active area of the OLED which was estimated to be 2 mm^2.

All the devices were encapsulated with glass lids and UV epoxy resin inside the inert atmosphere. The luminance-current-voltage characteristics were measured in an ambient environment using a Keithley 2400 source meter and Keithley 2000 multimeter connected to a calibrated Si photodiode. The external quantum efficiency was calculated assuming Lambertian emission distribution. The electroluminescence spectra were recorded by an Andor DV420-BV CCD spectrometer.

12. References

[1] F. Vögtle, P. Neumann, *Tetrahedron Lett.* **1969**, *60*, 5329–5334.
[2] R. S. Cahn, C. Ingold, V. Prelog, *Angew. Chem. Int. Ed.* **1966**, *5*, 385–415.
[3] P. Lennartz, G. Raabe, C. Bolm, *Isr. J. Chem.* **2012**, *52*, 171–179.
[4] P. Lennartz, G. Raabe, C. Bolm, *Isr. J. Chem.* **2012**, *52*, 171-179.
[5] C. Braun, S. Bräse, L. L. Schafer, *European Journal of Organic Chemistry* **2017**, *2017*, 1760-1764.
[6] W. Guo, *Org Biomol Chem* **2015**, *13*, 10285-10289.
[7] J. Xiao, X. K. Liu, X. X. Wang, C. J. Zheng, F. Li, *Organic Electronics* **2014**, *15*, 2763-2768.
[8] C. Braun, Ph.D. thesis, Karlsruhe Institute of Technology **2017**.
[9] M. Toda, Y. Inoue, T. Mori, *ACS Omega* **2018**, *3*, 22–29.
[10] C. Rosini, R. Ruzziconi, S. Superchi, F. Fringuelli, O. Piermatti, *Tetrahedron: Asymmetry* **1998**, *9*, 55–62.
[11] O. V. Dolomanov, L. J. Bourhis, R. J. Gildea, J. A. K. Howard, H. Puschmann, *J. Appl. Crystallogr.* **2009**, *42*, 339-341.
[12] G. Sheldrick, *Acta Crystallogr., Sect. A* **2008**, *64*, 112-122.
[13] G. Sheldrick, *Acta Crystallogr., Sect. C: Cryst. Struct. Commun.* **2015**, *71*, 3-8.
[14] N. G. Connelly, W. E. Geiger, *Chem. Rev.* **1996**, *96*, 877-910.
[15] G. A. Crosby, J. N. Demas, *J. Phys. Chem.* **1971**, *75*, 991-1024.
[16] W. H. Melhuish, *J. Phys. Chem.* **1961**, *65*, 229-235.
[17] N. C. Greenham, I. D. W. Samuel, G. R. Hayes, R. T. Phillips, Y. A. R. R. Kessener, S. C. Moratti, A. B. Holmes, R. H. Friend, *Chem. Phys. Lett.* **1995**, *241*, 89-96.
[18] M. J. Frisch, G. W. Trucks, H. B. Schlegel, G. E. Scuseria, M. A. Robb, J. R. Cheeseman, G. Scalmani, V. Barone, B. Mennucci, G. A. Petersson, H. Nakatsuji, M. Caricato, X. Li, H. P. Hratchian, A. F. Izmaylov, J. Bloino, G. Zheng, J. L. Sonnenberg, M. Hada, M. Ehara, K. Toyota, R. Fukuda, J. Hasegawa, M. Ishida, T. Nakajima, Y. Honda, O. Kitao, H. Nakai, T. Vreven, J. A. Montgomery Jr., J. E. Peralta, F. Ogliaro, M. Bearpark, J. J. Heyd, E. Brothers, K. N. Kudin, V. N. Staroverov, R. Kobayashi, J. Normand, K. Raghavachari, A. Rendell, J. C. Burant, S. S. Iyengar, J. Tomasi, M. Cossi, N. Rega, J. M. Millam, M. Klene, J. E. Knox, J. B. Cross, V. Bakken, C. Adamo, J. Jaramillo, R. Gomperts, R. E. Stratmann, O. Yazyev, A. J. Austin, R. Cammi, C. Pomelli, J. W. Ochterski, R. L. Martin, K. Morokuma, V. G. Zakrzewski, G. A. Voth, P. Salvador, J. J. Dannenberg, S. Dapprich, A. D. Daniels, Ö. Farkas, J. B. Foresman, J. V. Ortiz, J. Cioslowski, D. J. Fox, Gaussian Inc., Wallingford, CT, **2013**.
[19] C. Adamo, V. Barone, *J. Chem. Phys.* **1999**, *110*, 6158-6170.
[20] J. A. Pople, J. S. Binkley, R. Seeger, *Int. J. Quant. Chem. Symp.* **1976**, *10*, 1.
[21] M. Moral, L. Muccioli, W. J. Son, Y. Olivier, J. C. Sancho-García, *J. Chem. Theory Comput.* **2015**, *11*, 168-177.